



UCC

Coláiste na hOllscoile Corcaigh, Éire
University College Cork, Ireland

Department of Electrical and Electronic Engineering

Module EE4050 – BE Project

Final Report

Active Stabilisation of Motorcycle Roll Dynamics at Low Speeds

Author: Conor Healy – 116334906

Supervisor: Dr. Gordon Lightbody

Date of Submission: 10th April 2020

DECLARATION

This report was written entirely by the author, except where stated otherwise. The source of any material not created by the author has been clearly referenced. The work described in this report was conducted by the author, except where stated otherwise.

Signed: Conor Healy

Date: 10th April 2020

SUMMARY

This report documents the modelling, simulation, design, manufacture and control a self-balancing motorcycle. The purpose of this work was to help create a vehicle with the potential to solve the problems that society has with traffic flow and parking shortages. With increasing numbers of people travelling to work alone, the benefits of commuting to work via motorcycle have never been more apparent. Motorcycle's have the potential to shorten traffic queues and allow more vehicles to be parked in a given area. To make mass commuting to work via motorcycles possible, they must be made safe to use for most of the working population. Motorcycles are typically heavy, and people may struggle to support and balance the vehicle's weight, particularly smaller people and motorcycle riders who are recovering from and injury. So, to ensure that motorcycles suitable for use as commuter vehicles, reliable balance control must be developed.

This work focuses on steering control. This form of balance control varies the motorcycle's steering angle to counteract the fall of the vehicle. It was decided to focus on steering control because it was the least researched and most challenging method of motorcycle control at the time of writing. Stabilising a motorcycle at low speeds is particularly challenging because the gyroscopic forces from the wheels are absent. While modelling the motorcycle, the most suitable geometry for controllability was determined. For optimum steering control, a motorcycle should have a negative trail length, its centre of mass should be as low down and far forward as possible and its head tube angle should be as close to ninety degrees as possible. SolidWorks was used to design a test vehicle that conformed to these criteria. The geometry from the SolidWorks model was exported to MATLAB and Simulink to make the simulations as accurate as possible. A dual-extrusion 3D printer was used to manufacture the motorcycle. The controllers from MATLAB were implemented on the test vehicle. It was determined that the dynamics of these controllers were too fast, resulting in an unstable system. The difference in control requirements was most likely due to frictional forces and non-linearities that were not considered in the simulations. After several controller iterations, stationary balance control of the motorcycle was achieved, however stability was low and disturbance rejection was poor. Further study into controller architectures and design would be necessary before this control system could be considered safe for use by people.

The project was successful in achieving balance control of a stationary motorcycle. While completing this work, the author gained valuable experience with systems engineering and the model-based design approach and overall, the project was a very positive experience.

ACKNOWLEDGEMENTS

The author would like to thank Dr. Gordon Lightbody for his help, guidance and insight throughout the project. The help received from James Griffiths and Hilary Mansfield while ordering components was highly valuable. Michael O'Shea and Tim Power were extremely helpful mounting a sprocket to the steering motor and manufacturing the motorcycle's axles. Special thanks to Michael O'Shea for his assistance with the toothed belt drivetrain. Finally, the author is particularly grateful for the family support received while undertaking this project.

TABLE OF CONTENTS

| | |
|---|----|
| 1. Introduction and Objectives..... | 1 |
| 2. Background and Theory | 4 |
| 2.1. Stabilisation of Mechanical Systems | 4 |
| 2.1.1. The Stabilisation Process | 4 |
| 2.1.2. Examples of Mechanical Stabilisation | 5 |
| 2.1.3. Controller Architectures used for Mechanical Stabilisation | 5 |
| 2.2. Stabilisation of Motorcycle Roll Dynamics..... | 6 |
| 3. Motorcycle Modelling, Design and Simulation | 10 |
| 3.1. Model-Based Design Approach | 10 |
| 3.2. Mathematical Modelling of Motorcycle Dynamics | 11 |
| 3.2.1. Mathematical Model for Roll Dynamics | 11 |
| 3.2.2. Mathematical Model for Forward Dynamics | 14 |
| 3.2.3. Optimising the Roll Transfer Function for Control | 17 |
| 3.2.4. The Need for Adaptive Control | 17 |
| 3.3. Motorcycle Design and Manufacture | 18 |
| 3.3.1. Component Selection | 18 |
| 3.3.2. SolidWorks Design and Manufacture | 24 |
| 3.4. Control of the Simulink Model | 26 |
| 4. Experimental Implementation | 29 |
| 4.1. IMU Sensor Fusion and Testing..... | 29 |
| 4.2. Active Stabilisation of the Motorcycle Model..... | 32 |
| 5. Results..... | 33 |
| 5.1. Simulated Results | 33 |
| 5.2. Experimental Results | 34 |
| 6. Discussion of Results..... | 35 |
| 6.1. Discussion of Simulated Results | 35 |

| | |
|--|----|
| 6.2. Discussion of Experimental Results | 35 |
| 7. Ethics and Health and Safety..... | 36 |
| 7.1. Ethical Considerations | 36 |
| 7.2. Health and Safety Concerns | 37 |
| 8. Suggestions for Future Work..... | 40 |
| 9. Conclusions | 41 |
| 10. References..... | 42 |
| Appendix A: Links to Online Repositories..... | 49 |
| Appendix B: Continuous Time Phase Lead Controller Design Code..... | 50 |
| Appendix C: Matched Pole Zero Phase Lead Emulation Code | 51 |
| Appendix D: Discrete Time Phase Lead Controller Design Code..... | 52 |
| Appendix E: Risk Assessment | 53 |
| Appendix F: Logbook | 57 |

LIST OF FIGURES AND TABLES

| | |
|---|----|
| Figure 1.1: Means of Travel to Work in Ireland [12]. | 2 |
| Figure 1.2: Lit Motors C-1 [14]. | 2 |
| Figure 1.3: Proposed Motorcycle Stabilisation System. | 3 |
| Figure 2.1: A Basic Mechanical Stabilisation System featuring Digital Control. | 5 |
| Figure 2.2: An Inverted Pendulum [35]. | 7 |
| Figure 2.3: a) Honda's Riding Assist system featuring variable trail length [39], b) Yamaha MOTORiD utilising two-wheel steering [40], c) Lit Motor's gyroscopic stabilisation system [41]. | 8 |
| Figure 2.4: a) Single Phase Steering, b) Anti-Phase Steering, c) In Phase Steering [57]. | 9 |
| Figure 3.1: Linear Design Approach. | 10 |
| Figure 3.2: Model Based Design Approach. | 10 |
| Figure 3.3: Labelled 3D view of a Bicycle [10]. | 11 |
| Figure 3.4: Labelled Top View of a Bicycle [10]. | 11 |
| Table 3.1: List of Symbols for the Motorcycle Model. | 12 |
| Table 3.2: Additional Symbols for Steering System Model. | 13 |
| Table 3.3: Symbols for Drive System Model. | 14 |
| Table 3.4: Drive Motor Symbols. | 16 |
| Figure 3.5: Simulated Transient Roll Angle with Correct Velocity Tuning. | 18 |
| Figure 3.6: Simulated Transient Roll Angle with Incorrect Velocity Tuning. | 18 |
| Figure 3.7: a) Arduino MKR WiFi 1010 [58], b) Arduino MKR IMU Shield [59], c) Arduino MKR Motor Carrier [60], d) Arduino MKR Assembly. | 19 |
| Figure 3.8: Simulated Steering Gearbox Outputs. | 20 |
| Figure 3.9: Simulated Steering Motor Electrical Inputs. | 20 |
| Figure 3.10: a) Steering Motor [61], b) Steering Gearbox [62], c) Steering Potentiometer [63]. | 21 |
| Figure 3.11: Simulated Drive System Gearbox Outputs. | 21 |
| Figure 3.12: Simulated Drive Motor Electrical Inputs. | 22 |
| Figure 3.13: Simulated Drive System Power Plots. | 22 |
| Figure 3.14: Drive Motor [64] | 23 |
| Figure 3.15: Battery Holders [65] | 23 |

| | |
|---|----|
| Figure 3.16: SolidWorks Model. | 24 |
| Figure 3.17: Section View of SolidWorks Model. | 24 |
| Figure 3.18: Manufacture of the Motorcycle..... | 25 |
| Figure 3.19: Continuous Time Roll and Steering Root Locus Plots..... | 27 |
| Figure 3.20: Discrete Time Roll and Steering Root Locus Plots..... | 28 |
| Figure 4.1: A Complimentary Filter. | 29 |
| Figure 4.2: A Kalman Filter..... | 30 |
| Figure 4.3: IMU Test Rig..... | 30 |
| Figure 4.4: Plot of IMU Roll Angle and Potentiometer Angle versus Time..... | 31 |
| Figure 4.5: Revised Motorcycle Control Architecture. | 32 |
| Figure 5.1: Simulated Roll and Steering Plots. | 33 |
| Figure 5.2: Simulated Drive Plots. | 33 |
| Figure 5.3: Experimental Roll and Steering Plots. | 34 |

LIST OF ABBREVIATIONS

| | |
|------|------------------------------------|
| MIMO | Multi-input multi-output |
| ADC | Analogue to digital converter |
| DAC | Digital to analogue converter |
| PID | Proportional integral differential |
| LiPo | Lithium polymer |
| IC | Integrated circuit |
| FYP | Final year project |
| SFI | Science Foundation Ireland |

LIST OF SCIENTIFIC SYMBOLS

| | |
|----------------|--|
| φ | Roll angle [rad] |
| δ | Steering angle [rad] |
| v_x | Forward velocity [m s ⁻¹] |
| v_y | Lateral velocity [m s ⁻¹] |
| a | Horizontal distance between the centre of mass and rear axle [m] |
| b | Wheelbase [m] |
| c | Trail length [m] |
| h | Height of centre of mass [m] |
| λ | Head tube angle [rad] |
| m | Mass of motorcycle [kg] |
| g | Acceleration due to gravity [m s ⁻²] |
| τ_δ | Torque applied to the steering shaft [N m] |
| J_s | Steering moment of inertia [kg m ²] |
| $V_{A,s}$ | Steering motor armature voltage [V] |
| $I_{A,s}$ | Steering motor armature current [A] |
| $R_{A,s}$ | Steering motor armature resistance [Ω] |
| $L_{A,s}$ | Steering motor armature inductance [H] |
| $k_{m,s}$ | Steering motor machine constant [N m A ⁻¹] |
| $\omega_{m,s}$ | Steering motor angular velocity [rad s ⁻¹] |
| $\tau_{m,s}$ | Steering motor torque [N m] |
| $\omega_{g,s}$ | Steering gearbox angular velocity [rad s ⁻¹] |
| $\tau_{g,s}$ | Steering gearbox torque [N m] |
| $n_{g,s}$ | Steering gearbox gear ratio [] |
| $\eta_{g,s}$ | Steering gearbox efficiency [] |
| F_d | Force due to aerodynamic drag [N] |
| F_r | Force due to rolling resistance [N] |
| F_g | Force due to incline [N] |
| ρ_a | Density of air [kg m ⁻³] |

| | |
|----------------|--|
| C_d | Drag coefficient [] |
| A | Frontal area of motorcycle [m ²] |
| v_x | Forward velocity [m s ⁻¹] |
| v_a | Wind velocity [m s ⁻¹] |
| C_r | Rolling resistance coefficient [] |
| m | Mass of motorcycle [kg] |
| g | Acceleration due to gravity [m s ⁻²] |
| θ | Incline angle [rad] |
| F_v | Total force on drive system [N] |
| F_m | Motive force [N] |
| τ_m | Motive torque [N m] |
| τ_{axle} | Axle torque [N m] |
| J_{axle} | Drivetrain moment of inertia [kg m ²] |
| $V_{A,d}$ | Drive motor armature voltage [V] |
| $I_{A,d}$ | Drive motor armature current [A] |
| $R_{A,d}$ | Drive motor armature resistance [Ω] |
| $L_{A,d}$ | Drive motor armature inductance [H] |
| $k_{m,d}$ | Drive motor machine constant [N m A ⁻¹] |
| $\omega_{m,d}$ | Drive motor angular velocity [rad s ⁻¹] |
| $\tau_{m,d}$ | Drive motor torque [N m] |
| $\omega_{g,d}$ | Rear axle angular velocity [rad s ⁻¹] |
| $\tau_{g,d}$ | Rear axle torque [N m] |
| $n_{g,d}$ | Drive system gear ratio (including belt drive) [] |
| $\eta_{g,d}$ | Drive gearbox efficiency (including belt drive) [] |
| $K_{PL,c}$ | Continuous-time phase lead gain [unit varies with application] |
| $zero_{PL,c}$ | Continuous-time phase lead zero [rad s ⁻¹] |
| $pole_{PL,c}$ | Continuous-time phase lead pole [rad s ⁻¹] |
| $K_{PL,d}$ | Discrete-time phase lead gain [unit varies with application] |
| $zero_{PL,d}$ | Discrete-time phase lead zero [] |

| | |
|----------------------|---|
| $pole_{PL,d}$ | Discrete-time phase lead pole [] |
| ξ | Damping [] |
| ω_n | Natural frequency [rad s ⁻¹] |
| j | Complex operator [] |
| $\hat{\theta}_k$ | Filter angle estimate [rad] |
| α | Filter weighting coefficient [] |
| $\hat{\theta}_{k-1}$ | Previous filter angle estimate [rad] |
| a_k | Accelerometer angle measurement [rad] |
| ω_k | Gyroscope angular velocity measurement [rad s ⁻¹] |
| T_f | Filter sampling period [s] |
| θ_{pot} | Potentiometer angle [rad] |
| K_{pot} | Potentiometer gain [°] |
| ADC_{value} | Numerical value from ADC [] |
| m_r | Roll controller output [°] |
| e_r | Roll controller error [°] |
| m_s | Steering controller output [V] |
| e_s | Steering controller error [°] |
| k | Sample number [] |
| T_s | Controller sampling period [s] |

1. INTRODUCTION AND OBJECTIVES

Technology is evolving at an increasing rate with significant credit due to advances in automation and control enabling faster design, prototyping and production, all at a lower cost than previously possible. Comparable developments in computing, sensors and microelectronics platforms have enabled the implementation of a variety of control systems that until recently were not feasible due to technological and financial barriers. The widespread availability of microcontroller and sensor platforms has resulted in paradigm shift from classical controllers built from analogue electronics to control algorithms implemented in software on digital platforms. Digital control schemes offer the advantages of easier adjustability, transferability and the option to use machine learning algorithms that could not be implemented using analogue hardware [1]. Autonomous stabilisation of both electrical and mechanical systems has enabled rapid developments in areas such as electricity distribution, mobility aid, medical devices and transport.

Instability is inherent to any two-wheeled vehicle and despite the availability of mass produced motorcycles since 1894 [2], motorcycle stabilisation is still an active area of research today. Mainstream manufacturers have only begun to unveil concepts and prototypes in recent years [3]–[9]. The instability of a motorcycle is most noticeable at low speeds due to the reduced angular momentum of the wheels [10]. It is this angular momentum that produces the gyroscopic forces that stabilise the motorcycle while it is moving [11]. Riding a motorcycle with balance control would greatly reduce the probability of low speed accidents. This technology could also enable remote control parking allowing people who don't have the physical strength to push a motorcycle to use them on a daily basis. In addition, combining active stabilisation and autonomous driving technology could enable motorcycles to drop and collect their owners before driving themselves to a suitable parking location. This means finding parking in congested areas such as city centres need no longer be an issue. This is of particular benefit due to increasing population densities in urban areas where, the prospect of narrow-profiled two-wheel vehicles becoming more common could yield significant improvements in traffic flow and reduce parking shortages. To put this in context, a study from the central statistics office showed that in 2016, 62 % of people drove a car to work while only 4.2 % of people travelled as passengers [12]. Figure 1.1 shows the means of travel to work in Ireland between 1986 and 2016. It should be noted that this study did not consider whether people had dropped their children to school, etc. before driving to work.

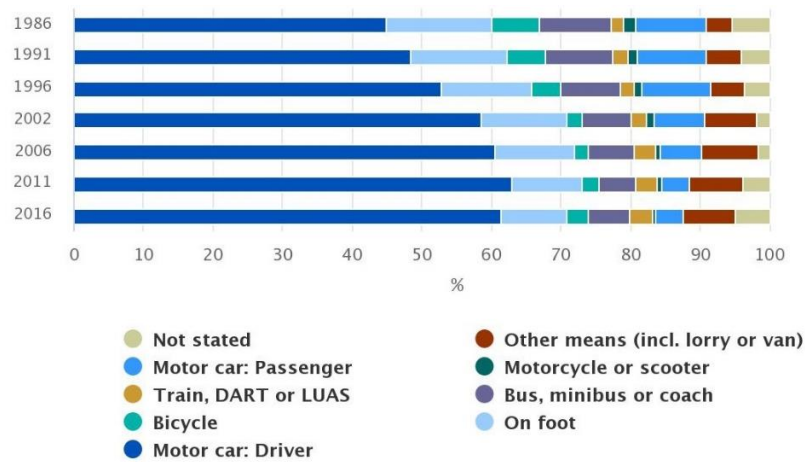


Figure 1.1: Means of Travel to Work in Ireland [12].

In addition to low speed instability, single track vehicles such as motorcycles also have the disadvantages of the rider being exposed to the elements and the steering, throttle and braking controls being vastly different to those in a car. These factors dissuade many people from driving motorcycles. In 2010 a San Francisco based start-up company Lit Motors [13] identified these issues and proposed a solution in the form of a gyroscopically stabilised two-wheeled vehicle (called the C-1) that featured a seat and steering wheel similar to a car. A picture of this vehicle with one of its doors removed can be seen in figure 1.2.



Figure 1.2: Lit Motors C-1 [14].

Stabilisation of motorcycle roll dynamics is achieved by counteracting the gravitational torque produced by the motorcycles centre of mass when it leans. The four main methods of generating this torque are moment gyroscopic control, inverted pendulum control, reaction wheel control and steering control [15]. Achieving stability using one of the first three methods, adds significant weight and volume to the motorcycle. Combining this with the high electrical energy requirement for these systems results in a vehicle with a much lower commuting range [10]. Steering control systems do not have the same power requirement because they manipulate the position of the motorcycle's centre of mass to vary and control the gravitational torque unlike the other systems which rely entirely on

electrical energy to generate a counter torque. In addition, steering control is the least researched of the three methods due to its additional complexity. With the exception of Honda's Riding Assist system [6]–[8] which operated by varying the trail length at the motorcycle's front wheel, robust steering control for stationary motorcycles has yet to be developed. Honda did not publish any technical details on this system [10] so the modelling and control techniques used remain largely unknown to the greater public.

The main objectives of this project were design a steering controlled balance system that could be integrated with a single-track vehicle. A scale model of a motorcycle featuring active balance stabilisation where the steering angle and trail length are the only control inputs will be built to test the system. The requirements for the control algorithm are that it would enable the motorcycle to balance while stationary and at low speeds in both forward and reverse directions. From a control perspective the motorcycle could be represented as a multi-input-multi-output (

MIMO) system where the inputs are the voltages applied to steering and drive motors and the measured outputs are the steering angle, roll angle and drive motor angular velocity. In addition, it was proposed that the velocity of the motorcycle could be wirelessly controlled via a smartphone application. A basic high-level diagram of the motorcycle stabilisation system can be seen in figure 1.3.

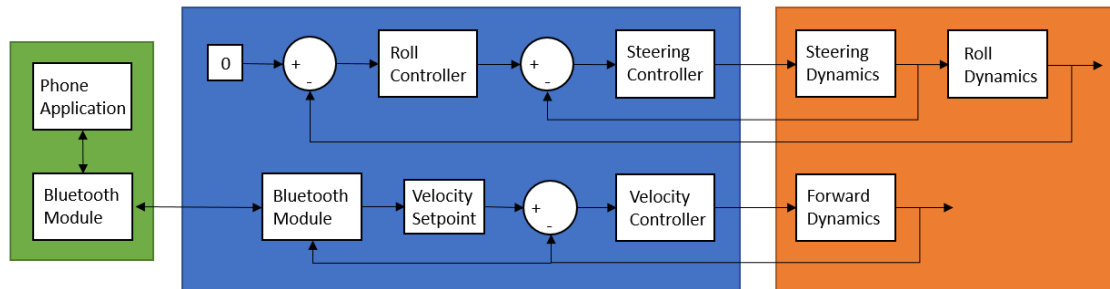


Figure 1.3: Proposed Motorcycle Stabilisation System.

2. BACKGROUND AND THEORY

2.1. STABILISATION OF MECHANICAL SYSTEMS

2.1.1. The Stabilisation Process

The purpose of stabilisation is to ensure the robustness and reliability of systems about their operating points. For a mechanical system this usually involves maintaining an equilibrium position by applying a controlled actuation or force. The stabilisation process usually consists of identifying the parameters that need to be stabilised (outputs) and varying other system parameters (inputs) to maintain a desirable output value [16]. A mathematical model known as a transfer function is used to relate output changes to input changes. A sensor measures deviations in the output from its operating point. A subtractor generates an error signal by comparing the setpoint with the output. The error signal is used as an input to the control algorithm which in turn sets the inputs to the mechanical system. Control systems are often influenced by disturbances. A disturbance is an external force or torque that acts on the system and affects its output [16]. Examples of disturbances are varying wind loads, adding mass to the system and a change in the load torque on an electric motor. For a control algorithm to function correctly, good disturbance rejection is crucial. There is often electrical noise and quantisation on the sensor outputs [17]. It is essential that the noise does not prevent the controller from stabilising the system.

While it is possible to implement control algorithms using only analogue electronics, digital control is more commonly used. Implementing the control algorithm on a computer offers access to a greater variety of control algorithms and simplifies the tuning of controller parameters [1]. However, a disadvantage of digital control is that it also increases system complexity. Mechanical systems are inherently analogue so an analogue to digital converter (ADC) and a digital to analogue converter (DAC) must be used to convert signals to and from the digital domain [1]. A sample and hold block is used in conjunction with the DAC to ensure the controller output voltage level is maintained for the duration of the controller's sampling period. A block diagram of a basic mechanical stabilisation system featuring digital control can be seen in figure 2.1.

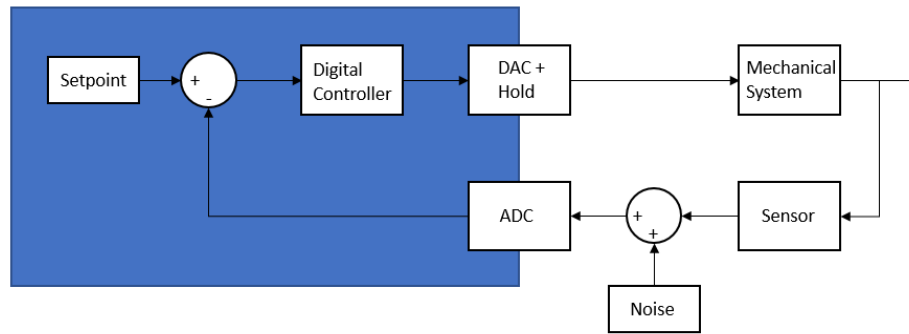


Figure 2.1: A Basic Mechanical Stabilisation System featuring Digital Control.

2.1.2. Examples of Mechanical Stabilisation

Many mechanical systems require autonomous stabilisation to ensure their safety and functionality. Many boats rely on anti-roll tanks or fin stabilisers to increase comfort and prevent them from capsising [18]. NASA uses a vehicle stabilisation system on its launch towers to counteract wind loads on space shuttles [19]. Some lorry trailers use sliders to stabilise them against crosswind disturbances [20]. Helicopters rely on the variation of the angle of attack of aerofoils as they rotate for steering and elevation control [21]. Stabilisation is also used in a wide variety of robotics and urban transport applications. Researchers at ETH Zurich [22] developed a cube that could jump up and balance on one of its edges or corners. The system used three reaction wheels and calliper brakes to generate the necessary torques for movement and stabilisation [23]. Flying robots such as drones also require precise control of pitch, roll and yaw angles for accurate coordinate control [24]. The Segway [25] two-wheeled inverted pendulum relies on precise control of its drive motors to remain upright. Actively stabilised single wheel transport systems such as the Ninebot by Segway [26] and the RYNO [27] have also been developed. While methods of actuation in these systems vary, they all rely on control algorithms for mechanical stabilisation.

2.1.3. Controller Architectures used for Mechanical Stabilisation

The dynamics caused by gravitational forces acting on stabilisation systems are typically fast. Therefore, to ensure good stability, controllers with short settling times are preferred. Examples of a variety of different controller architectures can be found in the literature. Classical control laws such as proportional integral differential (PID) controllers and phase lead compensators are easily designed in the Laplace or Z domains and can be used to shape the closed loop response of systems [1]. For these reasons, these controllers are often used as a first iteration before more advanced control schemes are considered. Cascade control systems are commonly used in DC motor speed control

because using an inner loop to control the motor torque in conjunction with the outer speed loop gives faster responses to changes in the speed setpoint [28]. Adaptive control schemes are useful for systems that have to operate under a range of conditions such as car suspensions where the mass of the vehicle and its centre of gravity can vary significantly depending on its occupancy [29]. State-space control techniques are useful for multi-input multi-output (MIMO) systems especially when the differential equations that model the system's dynamics are coupled [1]. In some cases, non-linear controllers have been used, for example researchers in [30] demonstrated the use of a nonlinear H_∞ control scheme to compensate for the approximation error in the linearisation of the asynchronous generator model of doubly fed induction motors.

2.2. STABILISATION OF MOTORCYCLE ROLL DYNAMICS

Autonomous control algorithms have made significant advancements in recent years enabling technologies that were once only be seen in science fiction to be used in everyday life. Many automotive manufacturers offer cars with autonomous features such as intelligent emergency braking, parking, overtaking, and even navigating a car park when summoned by their owner [31], [32]. Despite the increasing development of these technologies for four-wheel vehicles, similar products remain unavailable for single-track vehicles such as motorcycles. This is largely due to the added complexity of a motorcycle's inherent instability at low speeds. For motorcycles to feature technology comparable to that of four-wheeled vehicles, reliable balance control must first be achieved. Motorcycles offer several advantages over cars such as having a lower price and running cost, reduced energy consumption, a smaller parking space requirement and less contribution to traffic congestion. For this reason, it is equally important that balance control and autonomous driving technology be developed for motorcycles.

Before the stabilisation controllers can be designed, it is first necessary to derive a model that fully describes the motorcycle's dynamics [33], but for the purposes of introducing motorcycle stabilisation, a very basic mathematical model of roll dynamics is considered. Arguably the simplest way to model the roll dynamics of a stationary motorcycle is as an inverted pendulum hinged at the motorcycle's wheel-ground axis [34]. The motorcycle is in an unstable equilibrium when its centre of mass is directly above its base. Even the slightest rotation from this equilibrium position produces in a net torque that would cause the motorcycle to collapse. A basic inverted pendulum can be seen in figure 2.2.

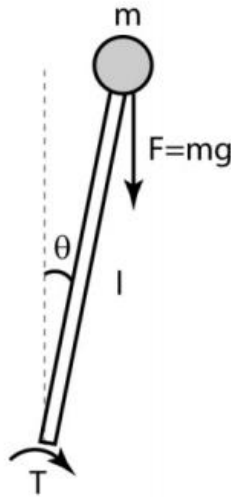


Figure 2.2: An Inverted Pendulum [35].

To stabilise the roll dynamics of a motorcycle a counter-torque is required to cancel the effects of the gravitational torque [36]. Several different methods of motorcycle stabilisation have been proposed and developed but they all share the common objective of generating this counter-torque.

Mainstream motorcycle manufacturers such as BMW, Honda and Yamaha have each developed different methods of balance control in recent years [4]–[9], but in each case limited technical details were published [10], [36]. Honda's Riding Assist system works by varying the trail length at the front wheel of the motorcycle. Positive trail length causes the motorcycle to lean in the direction that the front wheel is turned. This provides more responsive handling at most speeds but for stationary balance control negative trail is preferred as the motorcycle falls in the opposite direction to the rotation of the handlebars [10]. Honda's prototype switches to negative trail at speeds below 3 mph [37]. The main advantage of Honda's system was that it could be easily integrated with an existing production model [6], [7]. Yamaha's concept features two-wheel steering making its dynamics very different to traditional motorcycles with front-wheel steering. Lit Motors, a start-up company based in San Francisco developed a gyroscopically stabilised two wheel vehicle [13]. However, the additional weight of the gyroscopes significantly increased energy consumption resulting in reduced commuting range [38]. Figure 2.3 shows Honda's Riding Assist prototype, Yamaha's MOTOROiD and Lit Motor's gyroscopic stabilisation system.

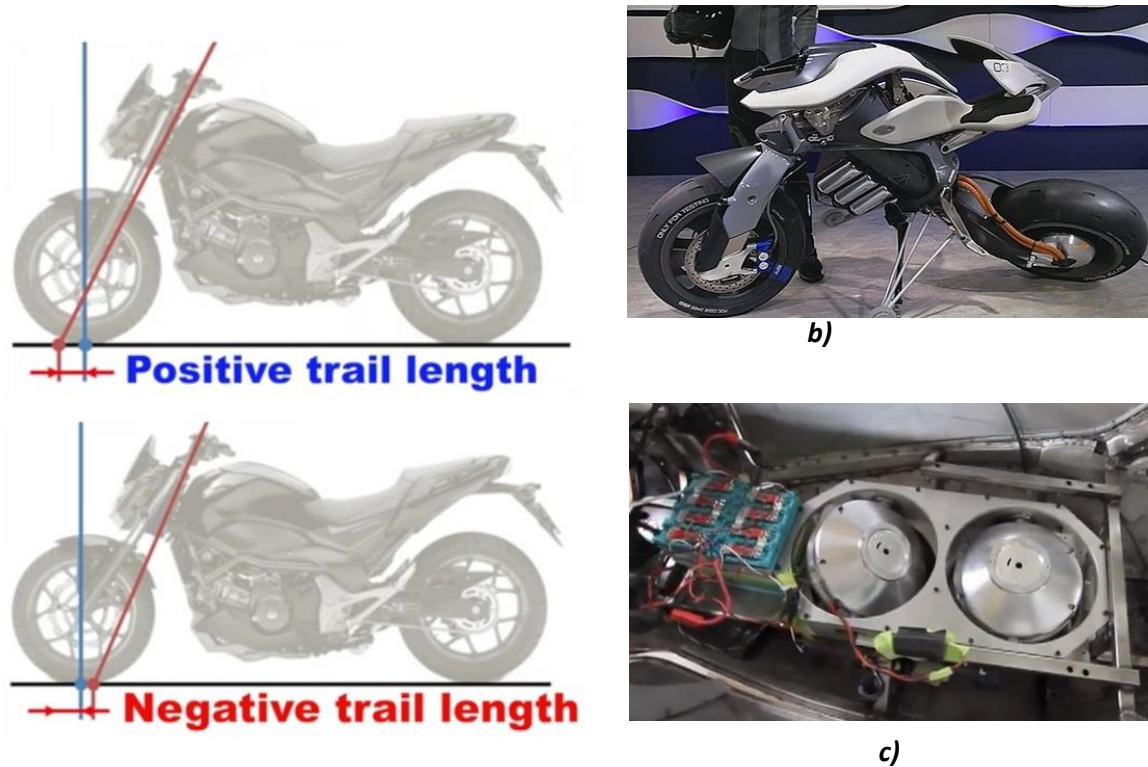


Figure 2.3: a) Honda's Riding Assist system featuring variable trail length [39], b) Yamaha MOTORiD utilising two-wheel steering [40], c) Lit Motor's gyroscopic stabilisation system [41].

BMW also experimented with autonomous driving technology on an R1200 GS [42]. The bike could navigate autonomously and park on a motorised side stand. However, this prototype featured no active stabilisation of roll dynamics, instead relying on the gyroscopic forces from the wheels to maintain balance while moving [43].

In the literature, several attempts have made to either enhance existing or develop new stabilisation techniques. When new systems are developed, it is often necessary to model the dynamics specific to that system. For this reason, mechanical modelling is as important to the stabilisation process as controller design. The first comprehensive model of motorcycle dynamics was developed in 1971 [44]. However, this model was highly non-linear and therefore not directly applicable to controller design. Therefore several linearised motorcycle models exist to facilitate the design of control systems [45]–[47].

Gyroscopically controlled systems achieve stability by using the angular momentum from a spinning gyroscope to counteract the fall of the motorcycle [48]. Inverted pendulum control systems rely on moving a mass within the motorcycle to change the position of its centre of mass to achieve balance control. The torque developed from this method is generally lower than using a gyroscope or reaction wheel making it more difficult to achieve stability [15]. Reaction wheel systems feature a spinning flywheel that generates a reaction torque to the motor that is driving it [49]. Stability is easily achieved

with a reaction wheel and this has been demonstrated in undergraduate studies [50], [51] and in an engineering kit released by Arduino [52]. Using a reaction wheel requires a large amount of volume on the motorcycle. While this is not a major issue for a bike-bot, fitting a rider and a reaction wheel on the same motorcycle becomes problematic.

Steering control requires less energy than the other three methods as the motorcycle's weight is being used to generate the counter torque instead of relying entirely on electrical energy [10]. However, this method has been less successful in stabilising motorcycle roll when compared with gyroscopic or reaction wheel control, with many studies failing to balance the motorcycle at stationary speeds where the gyroscopic stabilisation from the wheels is absent [34], [53]–[55]. In [10], the trail length was varied in a similar manner to Honda's system but stability at low speeds was not possible due to constraints on the feed-forward coefficient used in conjunction with the PID controller. Despite these failings, a small number of attempts have been successful in achieving balance control while stationary [56], [57]. The researchers in [57] also experimented with both anti-phase and in phase two-wheel steering, achieving better stability on both occasions at the cost of increased complexity and a greater deviation from standard motorcycle dynamics. For both papers, stability when using single phase steering was poor. For the purpose of clarity, single phase, anti-phase and in phase steering are shown in figure 2.4.

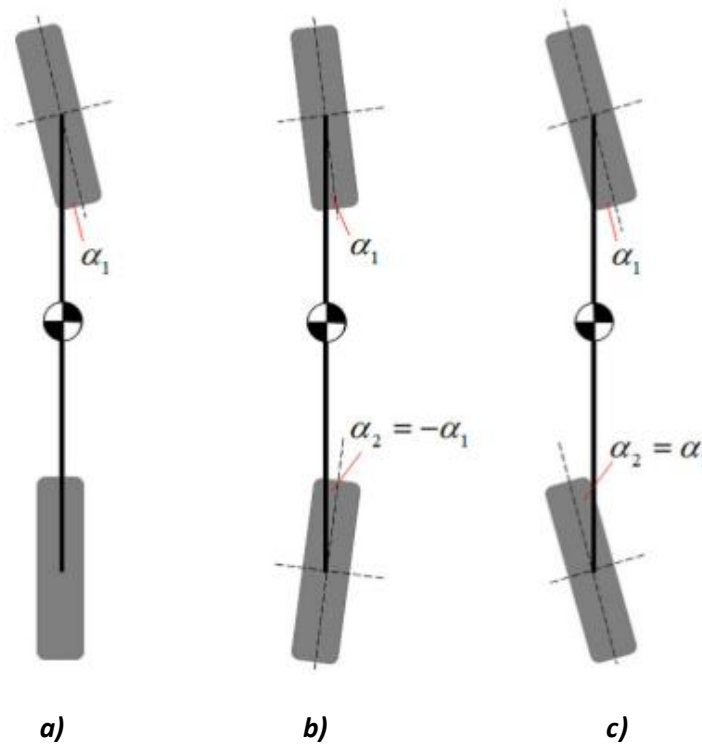


Figure 2.4: a) Single Phase Steering, b) Anti-Phase Steering, c) In Phase Steering [57].

3. MOTORCYCLE MODELLING, DESIGN AND SIMULATION

3.1. MODEL-BASED DESIGN APPROACH

During this project, a model-based design approach was used. In contrast to a linear design approach where each step of the design process is completed in series, the model-based design approach completes these steps iteratively and in parallel. Manufacture of components was also completed iteratively. Components were 3D printed, tested and redesigned if required. Instead building a motorcycle and then trying to control it, the model-based approach allowed the designer to design the motorcycle to be as controllable as possible. This was done by simulating the system model and checking how design changes affect performance. This approach proved vital when selecting the motors and gearboxes for the project, especially given the limited space available in the motorcycle's body. Another benefit of this approach was that it ensured that simulation results were as accurate as possible because the calculated model parameters from SolidWorks were used in the Simulink simulations meaning the values of the controller coefficients should be similar for the simulated and physical models. Linear and model-based design approaches can be seen in figures 3.1 and 3.2.

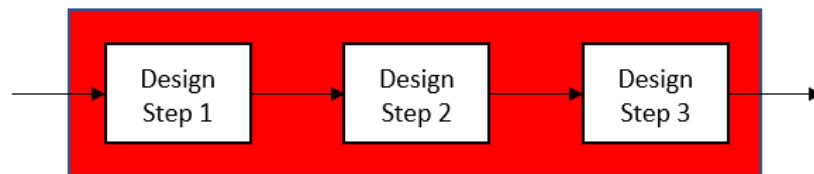


Figure 3.1: Linear Design Approach.

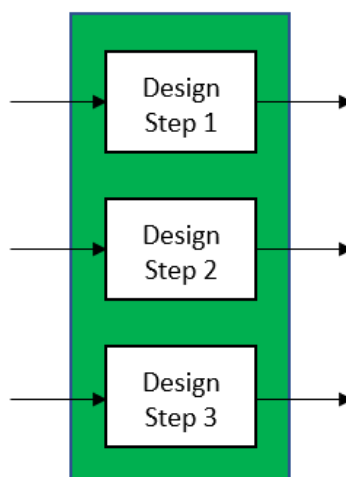


Figure 3.2: Model Based Design Approach.

3.2. MATHEMATICAL MODELLING OF MOTORCYCLE DYNAMICS

3.2.1. Mathematical Model for Roll Dynamics

The mathematical model used to describe the roll dynamics of the motorcycle in this project was obtained from [10]. As modelling was not the primary focus of this project, the model is not derived here. Instead, only the most important equations are shown. The various length and angle variables for the bicycle used in this model can be seen in figures 3.3 and 3.4. It should be noted that the roll dynamics of a bicycle and motorcycle are essentially the same.

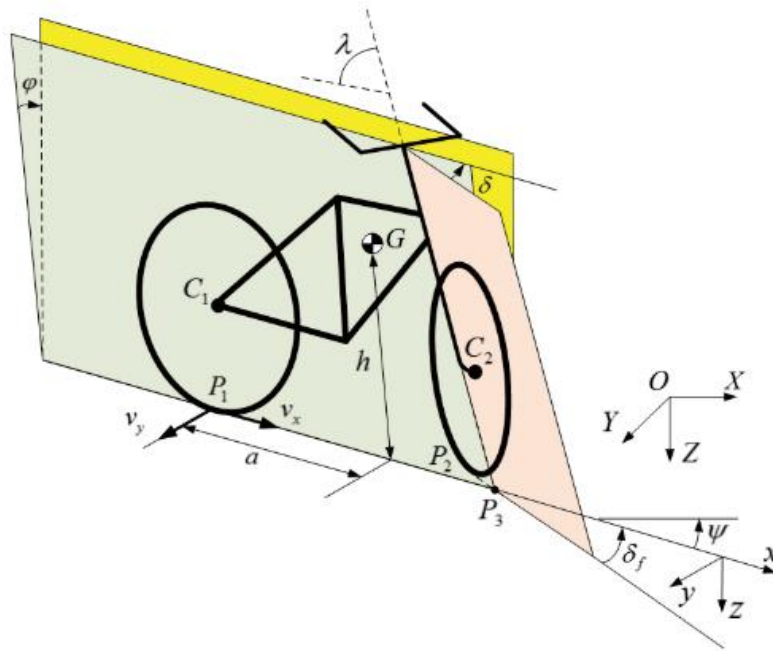


Figure 3.3: Labelled 3D view of a Bicycle [10].

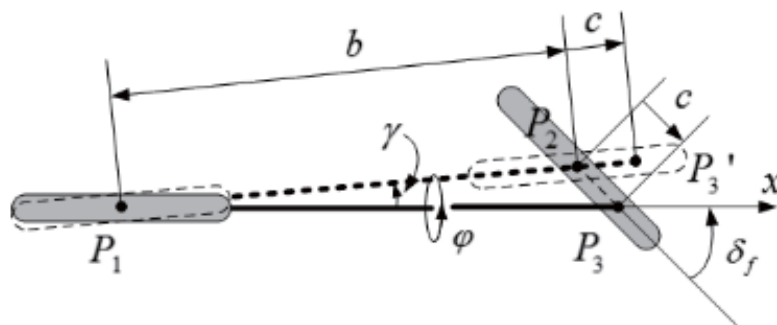


Figure 3.4: Labelled Top View of a Bicycle [10].

The symbols used in this model are explained in table 3.1.

| | |
|---------------|--|
| φ | Roll angle [rad] |
| δ | Steering angle [rad] |
| v_x | Forward velocity [m s ⁻¹] |
| v_y | Lateral velocity [m s ⁻¹] |
| a | Horizontal distance between the centre of mass and rear axle [m] |
| b | Wheelbase [m] |
| c | Trail length [m] |
| h | Height of centre of mass [m] |
| λ | Head tube angle [rad] |
| m | Mass of motorcycle [kg] |
| g | Acceleration due to gravity [m s ⁻²] |
| τ_δ | Torque applied to the steering shaft [N m] |
| J_s | Steering moment of inertia [kg m ²] |

Table 3.1: List of Symbols for the Motorcycle Model.

The nonlinear equations for the steering and roll dynamics were:

$$J_s \ddot{\delta} - \frac{macg \sin(\lambda) \sin(\varphi)}{b \cos(\varphi)} = T_\delta \quad \{3.1\} [10]$$

$$mh^2 \ddot{\varphi} + \frac{mah \sin(\lambda)}{b} \delta \dot{v}_x - mgh \sin(\lambda) + \frac{mah \sin(\lambda)}{b} \dot{\delta} v_x - \frac{macg \sin(\lambda)}{b \cos(\varphi)^2} \delta + \frac{mhv_x^2 \sin(\lambda) \delta}{b} \left(1 - \frac{h \delta \sin(\lambda) \sin(\varphi)}{b \cos(\varphi)}\right) + \frac{mahv_x \sin(\lambda) \sin(\varphi)}{b \cos(\varphi)} \delta \dot{\varphi} = 0 \quad \{3.2\} [10]$$

Assuming small forward accelerations and linearising gives:

$$J_s \ddot{\delta} - \frac{macg \sin(\lambda)}{b} \varphi = \tau_\delta \quad \{3.3\} [10]$$

$$mgh\varphi = mh^2 \ddot{\varphi} + \frac{mah \sin(\lambda)}{b} \dot{\delta} v_x + \left(\frac{mhv_x^2 \sin(\lambda)}{b} - \frac{macg \sin(\lambda)}{b} \right) \delta = 0 \quad \{3.4\} [10]$$

After taking a Laplace transform, the linear equation for roll dynamics can be rearranged to give the following transfer function:

$$\frac{\varphi(s)}{\delta(s)} = \frac{-s \frac{ah \sin(\lambda) v_x}{bh} + \frac{acg \sin(\lambda)}{bh^2} - \frac{\sin(\lambda) v_x^2}{bh}}{s^2 - \frac{g}{h}} \quad \{3.5\}$$

To fully model the steering system, it was necessary to include the steering motor and gearbox in the model. The additional symbols used in the steering system model can be seen in table 3.2.

| | |
|----------------|--|
| $V_{A,s}$ | Steering motor armature voltage [V] |
| $I_{A,s}$ | Steering motor armature current [A] |
| $R_{A,s}$ | Steering motor armature resistance [Ω] |
| $L_{A,s}$ | Steering motor armature inductance [H] |
| $k_{m,s}$ | Steering motor machine constant [N m A ⁻¹] |
| $\omega_{m,s}$ | Steering motor angular velocity [rad s ⁻¹] |
| $\tau_{m,s}$ | Steering motor torque [N m] |
| $\omega_{g,s}$ | Steering gearbox angular velocity [rad s ⁻¹] |
| $\tau_{g,s}$ | Steering gearbox torque [N m] |
| $n_{g,s}$ | Steering gearbox gear ratio [] |
| $\eta_{g,s}$ | Steering gearbox efficiency [] |

Table 3.2: Additional Symbols for Steering System Model.

The steering motor was modelled using the following differential equation for a permanent magnet DC machine:

$$V_{A,s} = R_{A,s} I_{A,s} + L_{A,s} \frac{dI_{A,s}}{dt} + k_{m,s} \omega_{m,s} \quad \{3.6\} [28]$$

After taking a Laplace transform and rearranging, equation {3.6} becomes:

$$I_{A,s}(s) = \frac{1}{(R_{A,s} + sL_{A,s})} (V_{A,s}(s) - k_{m,s} \omega_{m,s}(s)) \quad \{3.7\} [28]$$

The following two equations were used to relate the angular velocity and torque at the output of the gearbox to those of the motor.

$$\omega_{g,s} = \frac{\omega_{m,s}}{n_{g,s}} \quad \{3.8\} [28]$$

$$\tau_{g,s} = n_{g,s} \eta_{g,s} \tau_{m,s} \quad \{3.9\} [28]$$

Taking a Laplace transform of equation {3.3}, making the substitution:

$$\tau_\delta(s) = \tau_{g,s}(s) = k_{m,s} I_{A,s}(s) \quad \{3.10\} [28]$$

and using equations {3.8} and {3.9} allows the following transfer function to be derived:

$$\frac{\delta(s)}{V_{A,s}(s)} = \frac{\frac{n_{g,s} \eta_{g,s} k_{m,s}}{J_s L_{A,s}}}{s^3 + s^2 \frac{R_{A,s}}{L_{A,s}} + s \frac{n_{g,s}^2 \eta_{g,s} k_{m,s}^2}{J_s L_{A,s}}} \quad \{3.11\}$$

3.2.2. Mathematical Model for Forward Dynamics

The model for the drive system included forces due to aerodynamics, rolling resistance and inclination angle. While it is understood that aerodynamic forces are small at low speeds, they were included in the model for proof of concept. The symbols used in the drive system model can be seen in table 3.3.

| | |
|---------------|---|
| F_d | Force due to aerodynamic drag [N] |
| F_r | Force due to rolling resistance [N] |
| F_g | Force due to incline [N] |
| ρ_a | Density of air [kg m^{-3}] |
| C_d | Drag coefficient [] |
| A | Frontal area of motorcycle [m^2] |
| v_x | Forward velocity [m s^{-1}] |
| v_a | Wind velocity [m s^{-1}] |
| C_r | Rolling resistance coefficient [] |
| m | Mass of motorcycle [kg] |
| g | Acceleration due to gravity [m s^{-2}] |
| θ | Incline angle [rad] |
| F_v | Total force on drive system [N] |
| F_m | Motive force [N] |
| τ_m | Motive torque [N m] |
| τ_{axle} | Axle torque [N m] |
| J_{axle} | Drivetrain moment of inertia [kg m^2] |

Table 3.3: Symbols for Drive System Model.

The force due to aerodynamic drag is given by:

$$F_d = \frac{1}{2} \rho_a C_d A (v_x + v_a)^2 \quad \{3.12\} [28]$$

The rolling resistance force is:

$$F_r = C_r mg \quad \{3.13\} [28]$$

When the motorcycle is driving on an incline, the force due to gravity must also be considered. This is given by:

$$F_g = mg \sin(\theta) \quad \{3.14\} [28]$$

The total force on the drive system is then:

$$F_v = F_d + F_r + F_g \quad \{3.15\} [28]$$

The motive force required to drive the motorcycle is given by:

$$F_m = m \frac{dv_x}{dt} - F_v \quad \{3.16\} [28]$$

The motive torque required at the axle to generate this motive force can be calculated using:

$$\tau_m = F_m r \quad \{3.17\} [28]$$

In addition to the motive torque required to drive the vehicle, the torque required to spin the rotating parts within the drivetrain must also be considered. Therefore, the total axle torque is given by:

$$\tau_{axle} = \tau_m + J_{axle} \frac{1}{r} \frac{dv_x}{dt} \quad \{3.18\} [28]$$

Again, it was necessary to include a model for a permanent magnet DC machine to fully model the system. The symbols used for the drive motor can be seen in table 3.4.

| | |
|----------------|--|
| $V_{A,d}$ | Drive motor armature voltage [V] |
| $I_{A,d}$ | Drive motor armature current [A] |
| $R_{A,d}$ | Drive motor armature resistance [Ω] |
| $L_{A,d}$ | Drive motor armature inductance [H] |
| $k_{m,d}$ | Drive motor machine constant [N m A^{-1}] |
| $\omega_{m,d}$ | Drive motor angular velocity [rad s^{-1}] |
| $\tau_{m,d}$ | Drive motor torque [N m] |
| $\omega_{g,d}$ | Rear axle angular velocity [rad s^{-1}] |
| $\tau_{g,d}$ | Rear axle torque [N m] |
| $n_{g,d}$ | Drive system gear ratio (including belt drive) [] |
| $\eta_{g,d}$ | Drive gearbox efficiency (including belt drive) [] |

Table 3.4: Drive Motor Symbols.

In a similar manner to the steering system, the drive motor was modelled using a first order differential equation for a permanent magnet DC machine:

$$V_{A,d} = R_{A,d}I_{A,d} + L_{A,d} \frac{dI_{A,d}}{dt} + k_{m,d}\omega_{m,d} \quad \{3.19\} [28]$$

After taking a Laplace transform and rearranging, equation {3.19} becomes:

$$I_{A,d}(s) = \frac{1}{(R_{A,d} + sL_{A,d})} (V_{A,d}(s) - k_{m,d}\omega_{m,d}(s)) \quad \{3.20\} [28]$$

The following two equations were used to relate the angular velocity and torque at the rear axle to those of the motor.

$$\omega_{g,d} = \frac{\omega_{m,d}}{n_{g,d}} \quad \{3.21\} [28]$$

$$\tau_{g,d} = n_{g,d}\eta_{g,d}\tau_{m,d} \quad \{3.22\} [28]$$

Taking a Laplace transform of equation {3.18}, making the substitution:

$$\tau_{axle}(s) = \tau_{g,d}(s) = k_{m,d}I_{A,d}(s) \quad \{3.23\} [28]$$

and using equations {3.21} and {3.22} allows the following transfer function to be derived:

$$\frac{v_x(s)}{V_{A,d}(s)} = \frac{\frac{n_{g,d}\eta_{g,d}k_{m,d}r}{(r^2m + J_{axle})L_{A,d}}}{s^2 + s\frac{R_{A,s}}{L_{A,s}} + \frac{n_{g,d}^2\eta_{g,d}k_{m,d}^2}{(r^2m + J_{axle})L_{A,s}}} \quad \{3.24\}$$

3.2.3. Optimising the Roll Transfer Function for Control

Looking at the roll transfer function of equation {3.5}, it was possible to choose the motorcycle's dimensions to optimise the control of roll dynamics. For the sake of readability, the transfer function for the special case of $c < 0$ is shown here.

$$\frac{\varphi(s)}{\delta(s)} = \frac{-\left[s\frac{ah\sin(\lambda)v_x}{bh} + \frac{a|c|g\sin(\lambda)}{bh^2} + \frac{\sin(\lambda)v_x^2}{bh}\right]}{s^2 - \frac{g}{h}} \quad \forall \quad c < 0 \quad \{3.25\}$$

The larger the magnitude of the transfer function, the higher the sensitivity of the roll angle to the steering angle. This would yield increased controllability of the motorcycle. Firstly, negative trail length ($c < 0$) ensures that the three terms on the top of the transfer function are of the same polarity. Second, the lower the centre of gravity, the higher the controllability so $h \rightarrow 0$ is another design guideline. Controllability can be increased further if the centre of mass is as far forward as possible (i.e. $\frac{a}{b} \rightarrow 1$). Another method of increasing the sensitivity of the transfer function is to have the head tube as close to vertical as possible. Mathematically, this requires that $\sin(\lambda) \rightarrow 1 \Leftrightarrow \lambda \rightarrow \frac{\pi}{2}$.

3.2.4: The Need for Adaptive Control

The zero of the roll transfer function is given by:

$$s = \frac{-[a|c|g + hv_x^2]}{av_x} \quad \forall \quad c < 0 \quad \{3.25\}$$

Clearly, the location of this zero is dependent on the velocity of the motorcycle. This means that as the speed of the motorcycle changes, so too does the roll transfer function. When the transfer function changes, the controller must also change, hence adaptive control is required for this system. The need for adaptive control is illustrated graphically in figures 3.5 and 3.6.

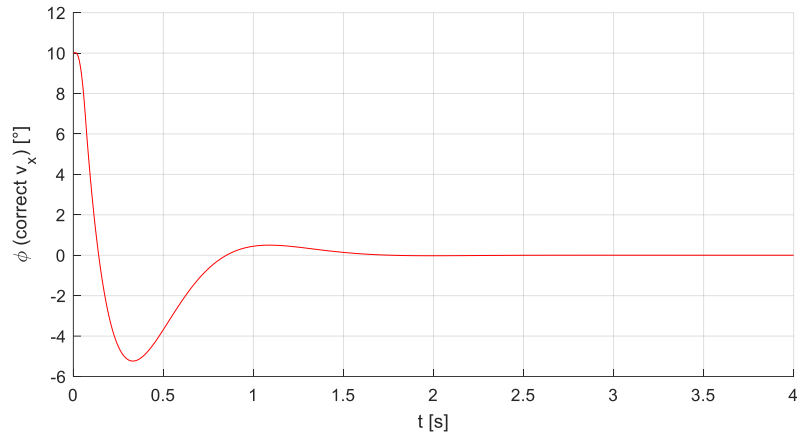


Figure 3.5: Simulated Transient Roll Angle with Correct Velocity Tuning.

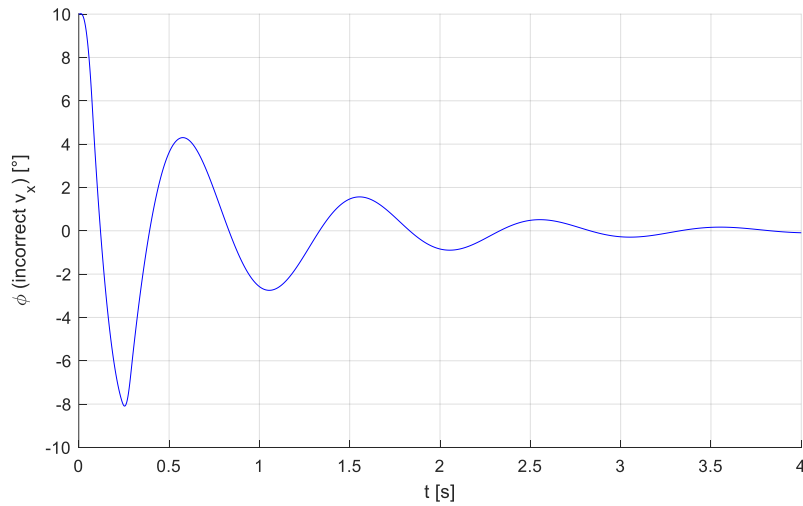


Figure 3.6: Simulated Transient Roll Angle with Incorrect Velocity Tuning.

In both cases, the motorcycle was driven at a speed of 0.15 m s^{-1} . In the top plot, the roll controller was tuned for this 0.15 m s^{-1} velocity, however in the bottom plot the controller was tuned to for a speed of 0.4 m s^{-1} . Peak overshoot, damping and settling time are adversely affected by incorrect controller tuning, hence the need for adaptive control.

3.3. MOTORCYCLE DESIGN AND MANUFACTURE

3.3.1. Component Selection

Before designing the model, it was necessary to choose the required electronic components so their dimensions could be factored into the design. The first components that were chosen were the microcontroller, IMU and motor shield because their voltage and current ratings would determine what motors could be used. It was decided to use the Arduino MKR 1010 WiFi with its accompanying

MKR IMU Shield and MKR Motor Carrier because the microcontroller featured a Bluetooth module that could communicate with a smartphone for remote control and the three components were designed to stack together. The Arduino components can be seen in figure 3.7

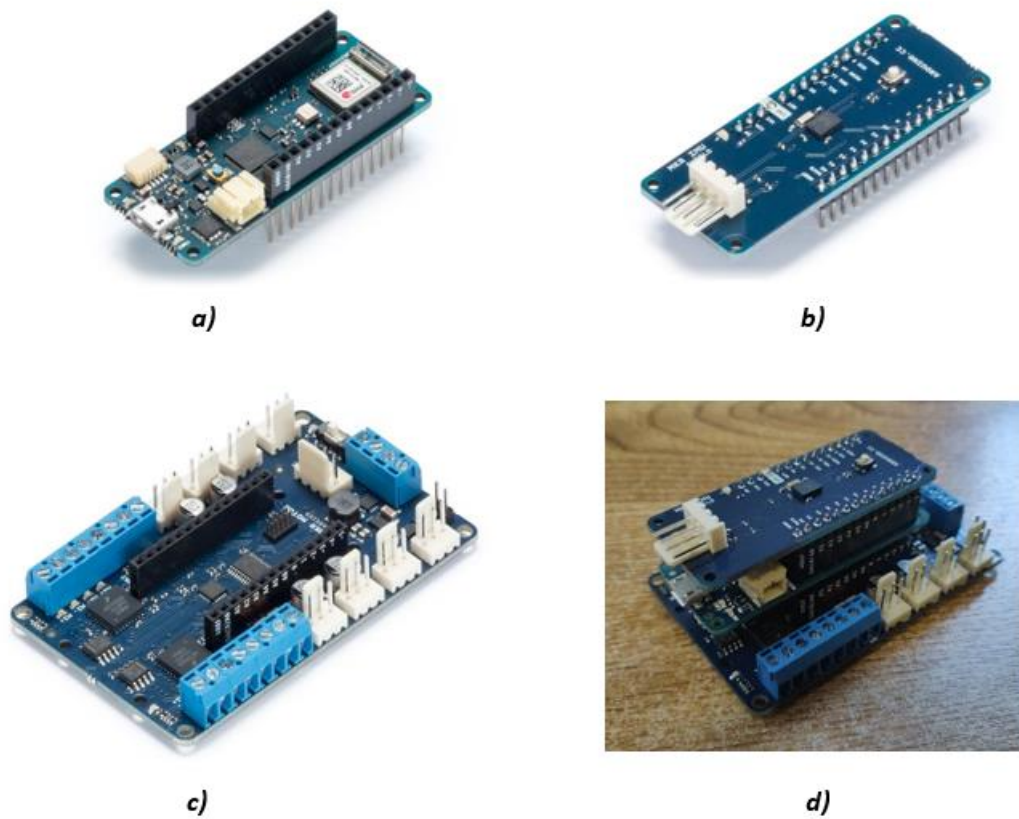


Figure 3.7: a) Arduino MKR WiFi 1010 [58], b) Arduino MKR IMU Shield [59], c) Arduino MKR Motor Carrier [60], d) Arduino MKR Assembly.

The next components to be chosen were the steering and drive motors. This proved to be quite challenging due to the power requirements of the control algorithms and the limited space available within the motorcycle's body. The model-based design approach was of particular use here, allowing several motors, gearboxes and supply limits to be simulated. The steering motor gearbox outputs for the steering system under analogue control can be seen in figures 3.8 and the steering motor's electrical plots can be seen in figure 3.9.

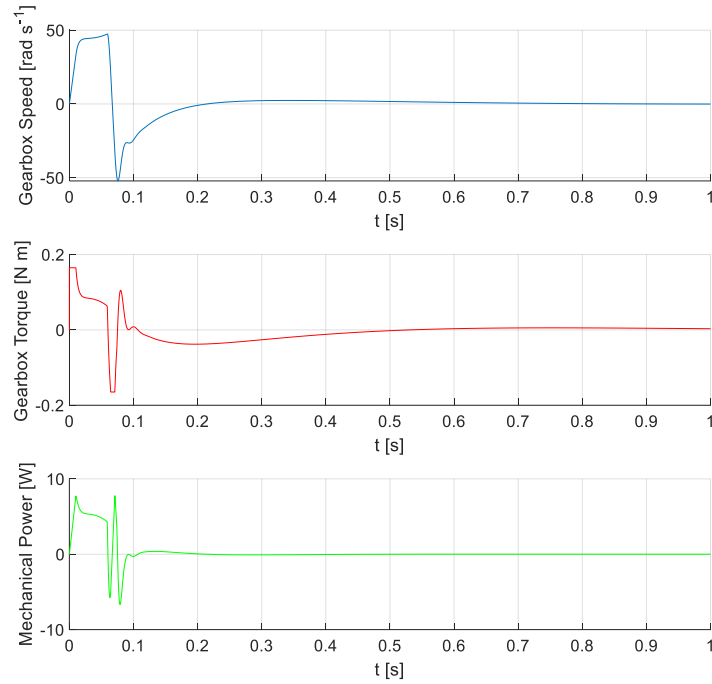


Figure 3.8: Simulated Steering Gearbox Outputs.

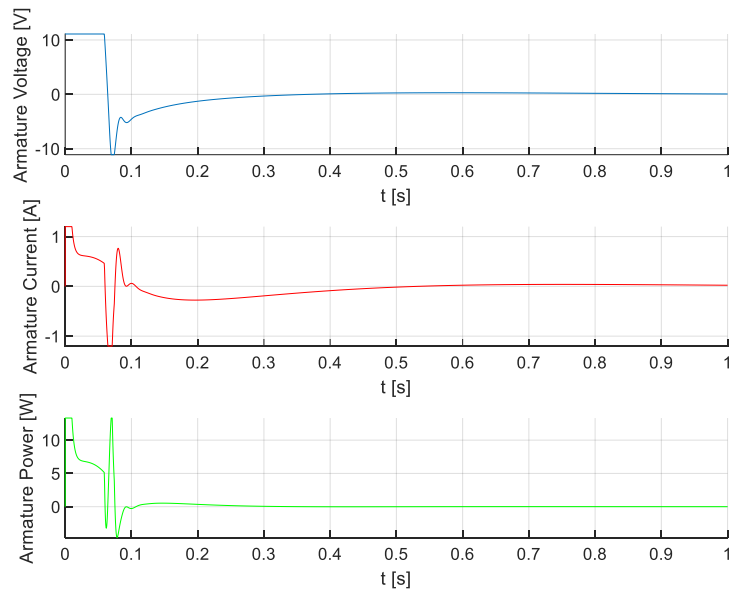


Figure 3.9: Simulated Steering Motor Electrical Inputs.

The purpose of these plots was to check that the motor and gearbox outputs were not saturated after the initial transient. Examples of saturation include, the back emf being greater than the supply voltage or the current limit being too low to deliver the required torque. Once all the responses were acceptable, the components for the steering system were chosen.

It was essential to have a steering motor and gearbox combination with fast dynamics and minimal backlash for accurate steering control. This meant that high quality (and expensive) components were

required for steering actuation. Based on the results from the Simulink simulations, a Portescap brushed DC motor (RS Stock No. 892-9120) and a McLennan Servo Supplies ovoid gearbox with a 25:1 gear ratio (RS Stock No. 336-444) were chosen. It was decided to use a metal rotary potentiometer with a long shaft to measure the steering angle because it would stabilise the rotation of the forks. The components for the steering system can be seen in figure 3.10.

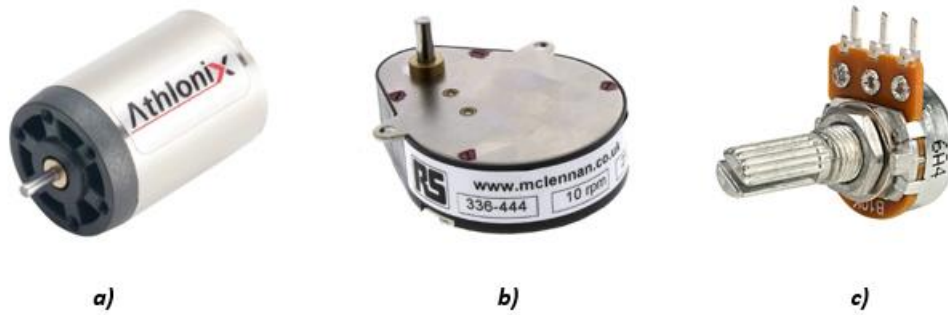


Figure 3.10: a) Steering Motor [61], b) Steering Gearbox [62], c) Steering Potentiometer [63].

The drive system was also simulated prior to component selection. The drive system gearbox outputs can be seen in figure 3.11, transient electrical plots can be seen in figure 3.12 and the motor's power plots can be seen in figure 3.13. Again, these plots were used to ensure that the transient responses of the motor were not saturated after the initial transient. After acceptable performance had been achieved, the drive motor was purchased.

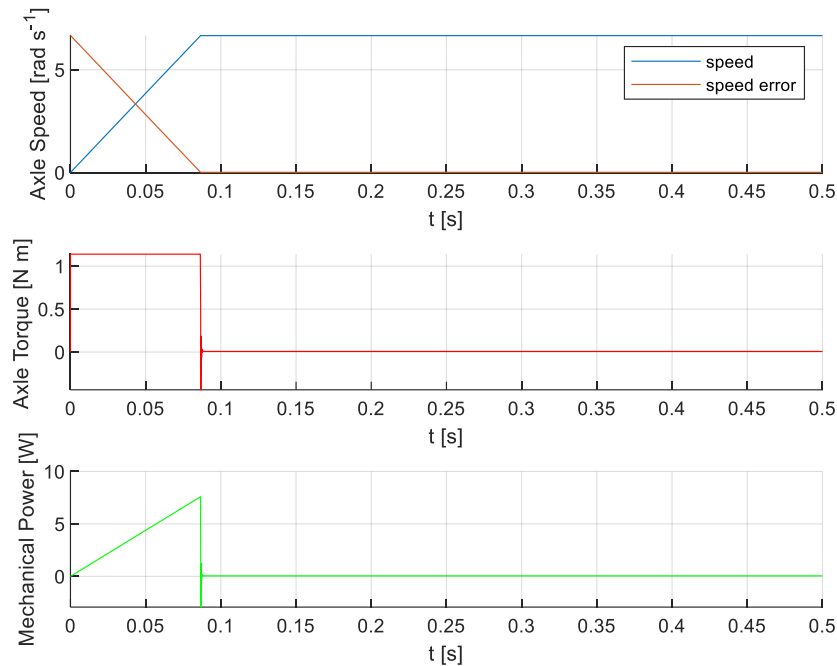


Figure 3.11: Simulated Drive System Gearbox Outputs.

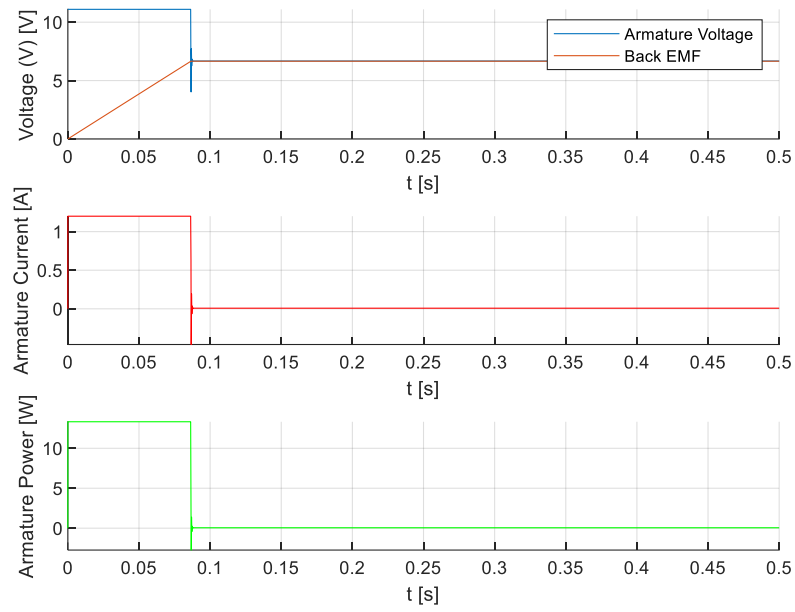


Figure 3.12: Simulated Drive Motor Electrical Inputs.

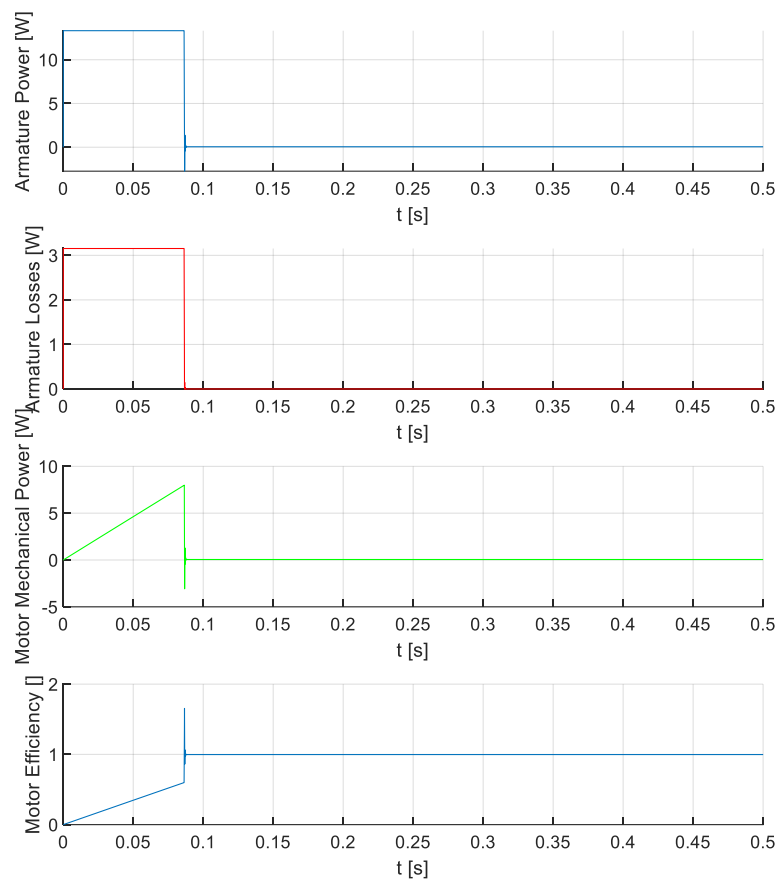


Figure 3.13: Simulated Drive System Power Plots.

The space for the drive motor was particularly limited and nothing suitable was available from UCC suppliers, so it was decided to use a small GA12-N20 permanent magnet motor from Amazon [64]. This motor also featured an encoder and can be seen in figure 3.14.



Figure 3.14: Drive Motor [64]

The final component to be chosen was the battery holder. Initially, a rechargeable lithium-ion battery pack was considered, but for the sake of increased reliability and fast battery changes on the open-day it was decided to use 8 AA batteries in series to obtain the required 12 V supply for the motor shield. As UCC's suppliers were out of stock at the time of purchase, this battery holder was also purchased from Amazon [65]. Two battery holders were purchased to facilitate faster battery changes. These can be seen in figure 3.15.

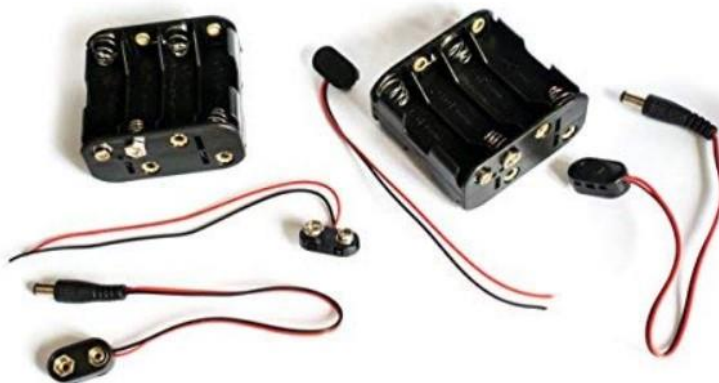


Figure 3.15: Battery Holders [65]

3.3.2. SolidWorks Design and Manufacture

The motorcycle was designed in accordance with the geometry guidelines of subsection 3.2.3. As a reminder, for optimum controllability the motorcycle should have its centre of mass as low down and far forward as possible, a negative trail length and head tube angle as close to vertical as possible. The SolidWorks model can be seen in figures 3.16 and 3.17.

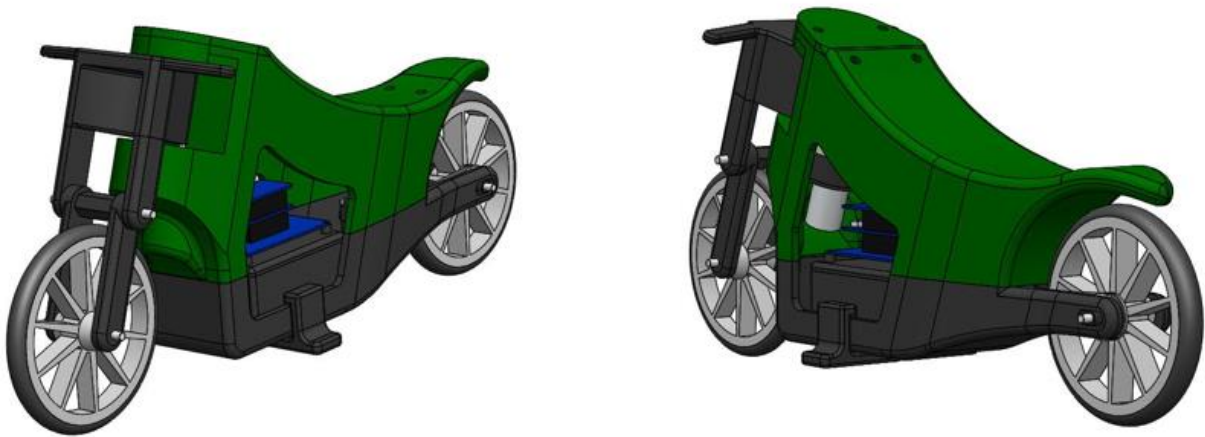


Figure 3.16: SolidWorks Model.

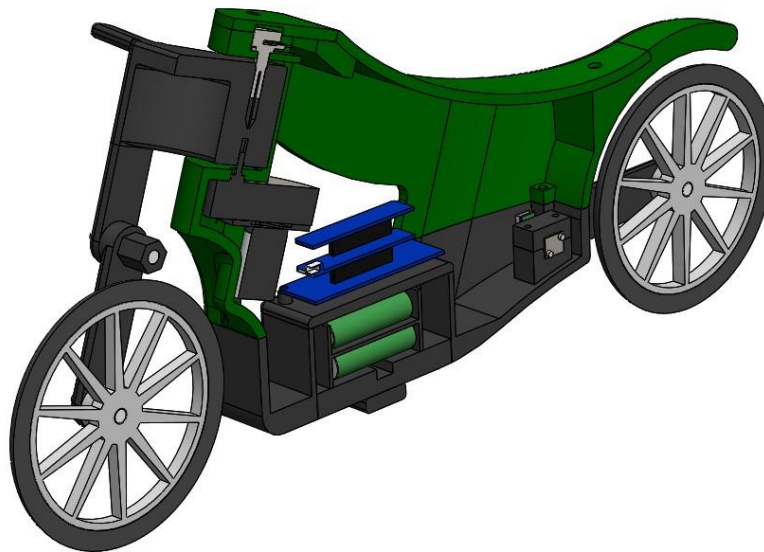


Figure 3.17: Section View of SolidWorks Model.

To make the motorcycle as controllable as possible, an ovoid gearbox was used in the steering system to allow the steering motor to be kept low down. The battery pack was also placed as low down and forward as possible without impeding access to the microcontroller's programming port. The top of the forks was hollowed out to remove any non-essential high-up mass. A pivoting fork was used to allow the trail length of the motorcycle to be varied. When the fork was straight, the trail length was

-20 mm. A head tube angle of 70° was chosen because going closer to 90° would have caused the front wheel to collide with the body of the motorcycle.

The design also included wheel bearings and steel axles to minimise lateral rocking of the wheels. This lateral movement could have made the system uncontrollable. A toothed belt drive was used for power transmission to the rear wheel.

The motorcycle was designed so that most of its parts could be 3D printed. The majority of these parts were 3D printed using a rigid PLA material, however the tires were printed from a flexible TPU to increase traction. Water soluble support materials enabled fast support removal after printing. Metal parts were used where the strength of 3D printed plastic was not sufficient. A selection of images of the motorcycle being manufactured can be seen in figure 3.18.

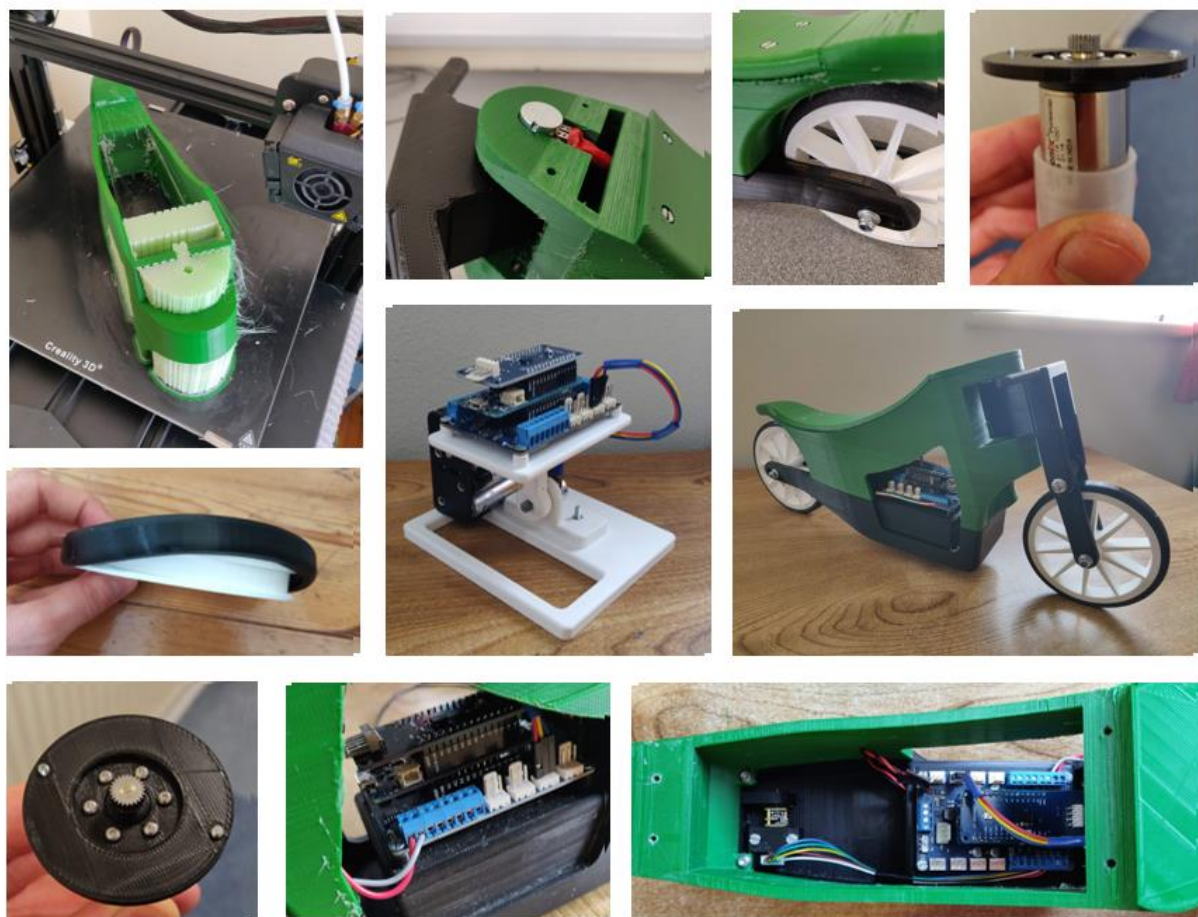


Figure 3.18: Manufacture of the Motorcycle.

3.4. CONTROL OF THE SIMULINK MODEL

Using the geometry and component densities from the SolidWorks model, it was possible to accurately calculate the parameters for the Simulink model. While analogue controllers were used for component selection and geometry testing, this section of the report focuses on digital control laws that could be implemented on an Arduino. As the 10 ms sampling period used on the Arduino was much faster than the dynamics of the motorcycle system, emulation of an analogue controller to the digital domain was possible. Phase lead controllers were used for the steering and roll systems and a proportional controller was used for the drive system. Continuous time (analogue) and discrete time (digital) phase lead controller equations can be seen in equations {3.26} and {3.27}.

$$C(s) = \frac{K_{PL,c}(s - zero_{PL,c})}{(s - pole_{PL,c})} \quad \{3.26\} [1]$$

$$D(z) = \frac{K_{PL,d}(z - zero_{PL,d})}{(z - pole_{PL,d})} \quad \{3.27\} [1]$$

The analogue controller was designed using the root locus method. The root locus allows the designer to place the controller poles and zeros to achieve desired controller performance while also checking the system's stability. The first step in this process is to choose desired values of closed-loop natural frequency and damping. Here both systems had 0.707 damping. The natural frequencies of the roll and steering systems were 12 rad s⁻¹ and 75 rad s⁻¹ respectively. The desired point on the root locus for a second order dominant system is given by:

$$s_{desired} = \xi\omega_n[-1 + j\tan(\cos^{-1}(\xi))] \quad \{3.28\} [1]$$

where ξ is the damping, ω_n is the natural frequency and j is the complex operator. The zero of the phase lead controller was then placed directly under the desired point. Any point on the root locus must satisfy a cascade of the controller and the open loop transfer function having a magnitude of 1 and a phase of -180°. The pole of the phase lead controller was placed to give the required -180° phase. Finally, the gain of the controller was chosen so the magnitude of the open-loop system was one at the desired point. Explaining the mathematics involved in these steps would cause the report to exceed its page limit, but for more detail the reader is referred to the MATLAB function "ctime_PL.m" in Appendix B. The resulting root locus plots for the roll and steering systems can be seen in figure 3.19.

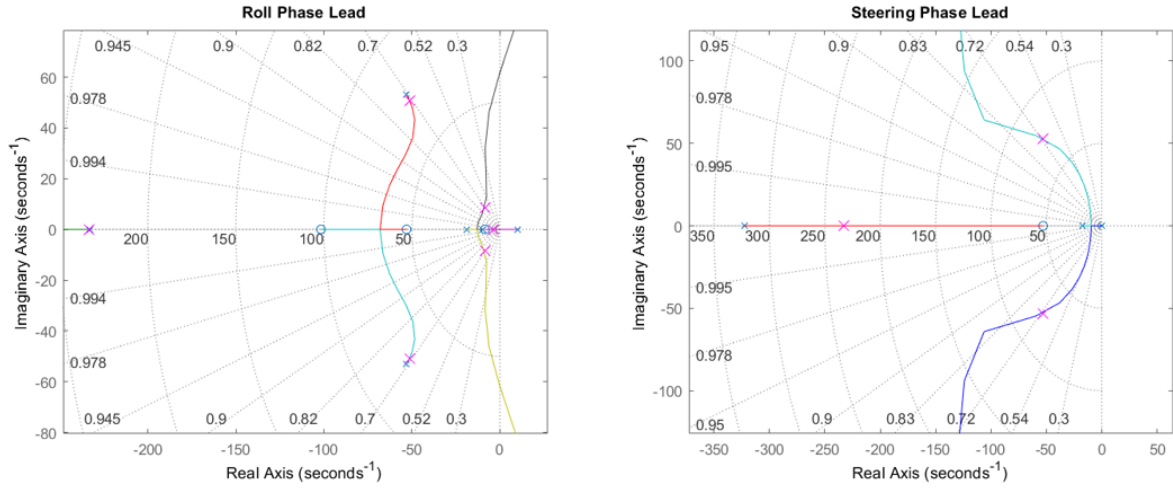


Figure 3.19: Continuous Time Roll and Steering Root Locus Plots.

For a continuous-time controller to be stable all closed loop poles (marked by a magenta X) must be in the left-hand side of the s-plane. Looking at the plots, this is clearly the case. The phase lead equations for these controllers were:

$$C_{roll}(s) = \frac{-21.1(s + 8.48)}{(s + 18.6)} \quad \{3.29\}$$

$$C_{steering}(s) = \frac{30.0(s + 53.0)}{(s + 17.7)} \quad \{3.30\}$$

Emulation from continuous to discrete controllers was done using the matched pole-zero method. In this method s-domain poles and zeros are mapped to the z-domain using the relations:

$$zero_{PL,d} = e^{zero_{PL,c}T_s} \quad \{3.31\} [1]$$

$$pole_{PL,d} = e^{pole_{PL,c}T_s} \quad \{3.32\} [1]$$

where T_s is the sampling period of the discrete time controller. The discrete time controller gain was chosen so that the DC gain was the same as the continuous version. This was calculated using:

$$K_{PL,d} = K_{PL,c} \frac{\lim_{s \rightarrow 0} \frac{(s - zero_{PL,c})}{(s - pole_{PL,c})}}{\lim_{z \rightarrow 1} \frac{(z - zero_{PL,d})}{(z - pole_{PL,d})}} \quad \{3.33\} [1]$$

The function used to implement the discussed emulation is called "MPZ_PL.m". It can be seen in Appendix C. Alternatively, a full-digital design can be utilised. While this is not discussed here due to

page limits, the design approach can be seen in the MATLAB function "dtime_PL.m" in Appendix D. The discrete time root locus plots for the roll and steering systems can be seen in figure 3.20.

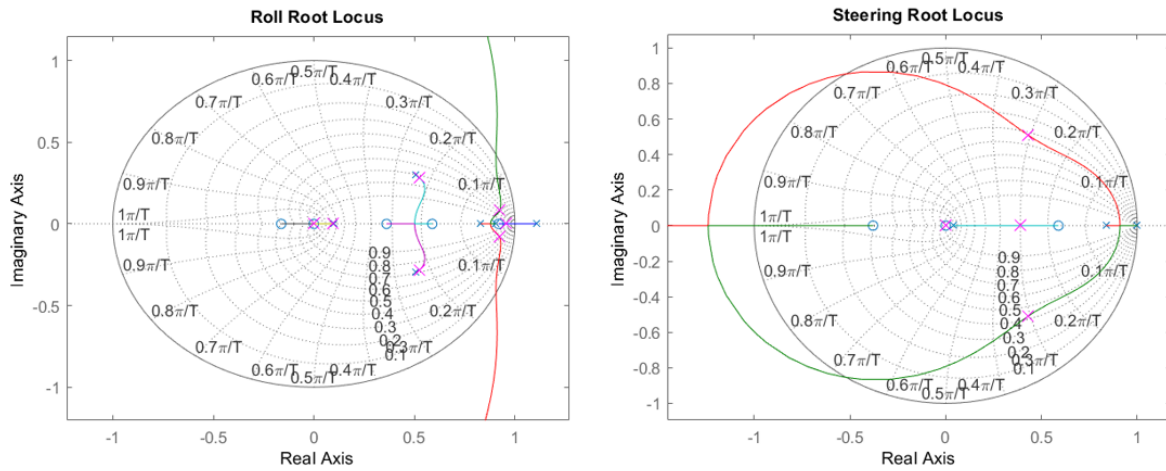


Figure 3.20: Discrete Time Roll and Steering Root Locus Plots.

For a discrete-time controller to be stable all closed loop poles (marked by a magenta X) must be inside the unit circle. Looking at the plots, this is clearly the case. The phase lead equations for these controllers were:

$$D_{roll}(z) = \frac{-20.1(z - 0.919)}{(z - 0.830)} \quad \{3.34\}$$

$$D_{steering}(z) = \frac{35.5(z - 0.588)}{(z - 0.838)} \quad \{3.35\}$$

A proportional controller gain of 25 was chosen for the drive system as it gave a fast response time without causing excessive saturation of the drive motor voltage output. The simulation results obtained with these controllers will be shown in section 5.

4. EXPERIMENTAL IMPLEMENTATION

4.1. IMU SENSOR FUSION AND TESTING

To ensure good stability when using digital control, it is essential to choose a microcontroller with appropriate specifications for the task at hand. Digital control systems can become unstable if the sampling period is too large relative to the time constant of the system or if there is a time delay in controller actuation [1]. For this reason, it is essential that the clock frequency of the microcontroller is high enough. Analogue data from the mechanical system is quantised by the microcontroller's ADC. Quantisation occurs when a continuous range of data is converted to a discrete range of data [1]. The number of discrete values (and the voltage difference between them) depends on the resolution (number of bits) of the ADC. If the quantisation becomes significant compared to the deviations in the sensor output, the signal to noise ratio of the system will suffer. This could lead to instability. Another important consideration when choosing a microcontroller platform is that it has enough memory and storage to run the control algorithm effectively.

High precision and accuracy of sensor data is highly important for the reliability of control systems. In a typical IMU, the accelerometer output suffers from high frequency noise while the gyroscope is prone to drift. Sensor fusion is necessary to get an accurate angle estimate. This involves combining the outputs of the accelerometer and gyroscope via signal processing techniques [66]. Two methods of doing this are using a complimentary filter or using a Kalman filter. The complementary filter works by low-pass filtering the accelerometer angle output to remove the noise and integrating and high-pass filtering the gyroscope angular speed signal to remove the drift. A block diagram for a complimentary filter can be seen in figure 4.1.

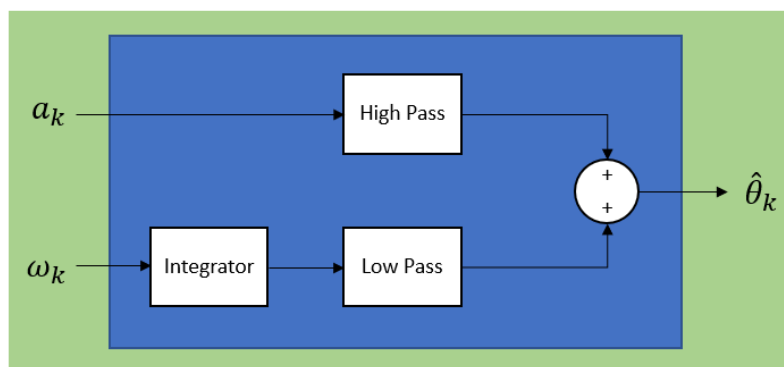


Figure 4.1: A Complimentary Filter.

The Kalman filter has simpler implementation, using only a weighted sum of the raw accelerometer and gyroscope signals and feedback of the previous angle estimate. A block diagram of a Kalman filter can be seen in figure 4.2.

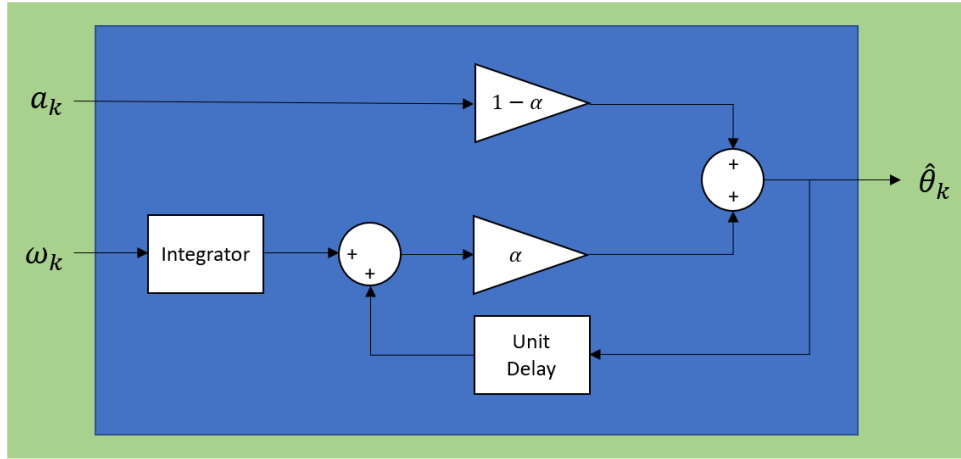


Figure 4.2: A Kalman Filter.

It can be shown that both filters yield the same update equation [66]:

$$\hat{\theta}_k = \alpha \hat{\theta}_{k-1} + (1 - \alpha)a_k + \alpha \omega_k T_f \quad \{4.1\} [66]$$

where $\hat{\theta}_k$ is the filter output, α is a weighting coefficient, $\hat{\theta}_{k-1}$ is the previous filter output, a_k is the accelerometer signal, ω_k is the gyroscope signal and T_f is the sampling period of the filter. Before manufacturing the physical model, the IMU was tested to better understand its performance. During this testing, it was determined that the Arduino MKR IMU shield came with in-built sensor fusion. The IMU output was compared with that of a rotary potentiometer to check the accuracy of this filter. This was done using an IMU test rig, which can be seen in figure 4.3.

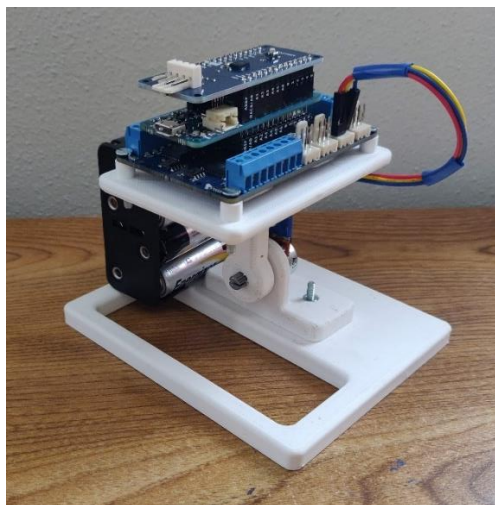


Figure 4.3: IMU Test Rig.

The ADC reading from the potentiometer was converted to an angle measurement using the following first order equation:

$$\theta_{pot} = K_{pot} (ADC_{value} - ADC_{value(\theta_{pot}=0)}) \quad \{4.2\}$$

where the gain K_{pot} was calculated using:

$$K_{pot} = \frac{70}{ADC_{value(\theta_{pot}=70)} - ADC_{value(\theta_{pot}=0)}} \quad \{4.3\}$$

The roll angle estimation from the IMU and the angle measurement from the potentiometer were graphed on the same plot. The sampling period was 10 ms. This result can be seen in figure 4.4.

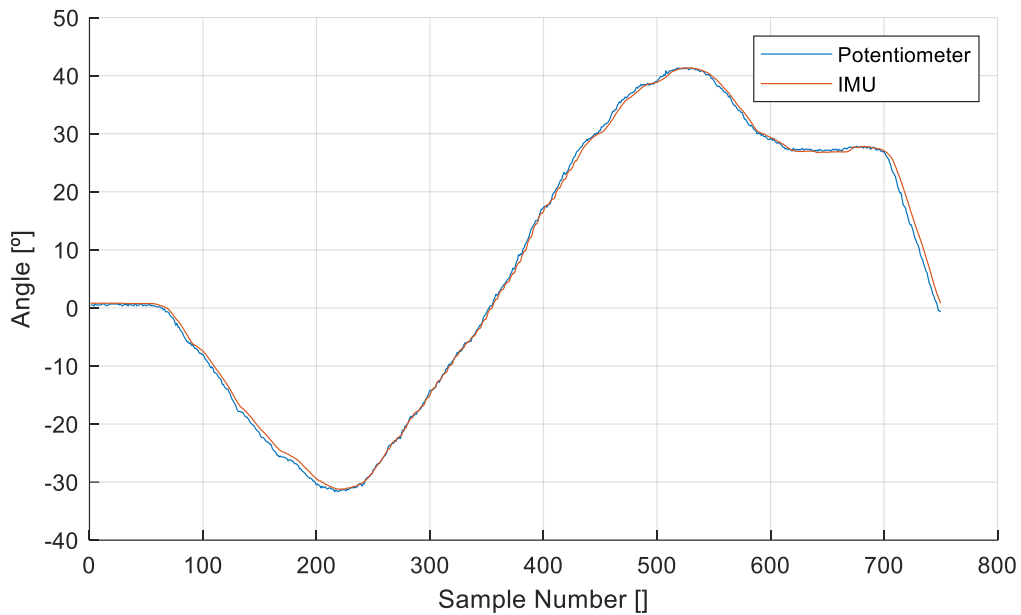


Figure 4.4: Plot of IMU Roll Angle and Potentiometer Angle versus Time.

Looking at figure 4.4, the IMU angle lagged the potentiometer angle when angular velocity was high. This was to be expected due to calculation time. Any steady-state error that was present was most likely due to potentiometer calibration. Despite these discrepancies it was decided that the performance of the inbuilt filter was adequate for use on the motorcycle. This meant that a new filter design was not required.

4.2. ACTIVE STABILISATION OF THE MOTORCYCLE MODEL

Initially it was hoped that once stable balance control had been achieved there would be time to build an app that would allow for remote control of the motorcycle. However, due to complications and delays with manufacture and achieving stable balance control this was no longer realisable. The control architecture for the motorcycle model was changed from that of figure 1.3 to the architecture shown here in figure 4.5.

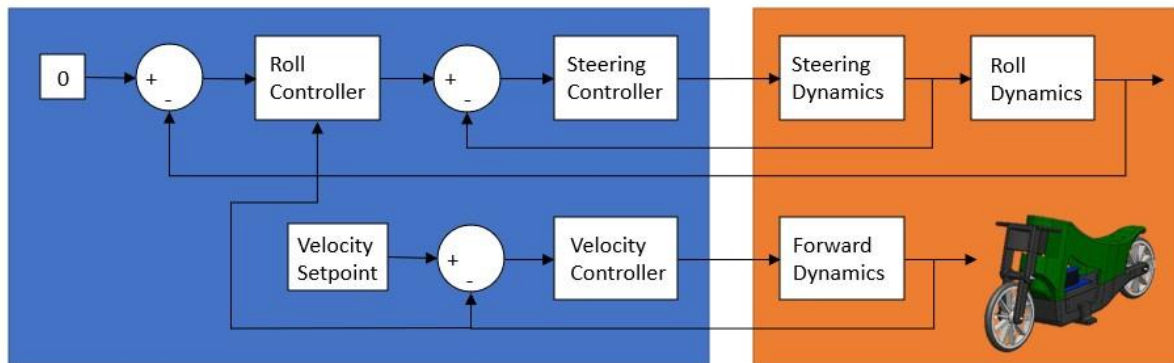


Figure 4.5: Revised Motorcycle Control Architecture.

Before the discrete time phase lead controllers could be coded on the Arduino microcontroller, they had to be implemented as difference equations. These difference equations were of the form.

$$m(kT_s) = K_{PL}[e(kT_s) - zero_{PL}e([k - 1]T_s)] + pole_{PL}m([k - 1]T_s) \quad \{4.4\} [1]$$

where m is the controller output, e is the error signal received by the controller and k is the sample number. T_s is the controller sampling period as before. After many design iterations for tuning the controllers, stable balance control of the motorcycle was achieved with the following controller difference equations for the roll and steering systems.

$$m_r(kT_s) = -7.78[e_r(kT_s) - 0.926e_r([k - 1]T_s)] + 0.987m_r([k - 1]T_s) \quad \{4.5\}$$

$$m_s(kT_s) = 8.17[e_s(kT_s) - 0.899e_s([k - 1]T_s)] + 0.993m_s([k - 1]T_s) \quad \{4.6\}$$

The results obtained with these controllers will be shown in section 5.

5. RESULTS

5.1. SIMULATED RESULTS

The Simulink model was run using the discrete-time phase lead controllers that were designed in subsection 3.4. The roll angle, steering angle and steering motor voltage can be seen in figure 5.1.

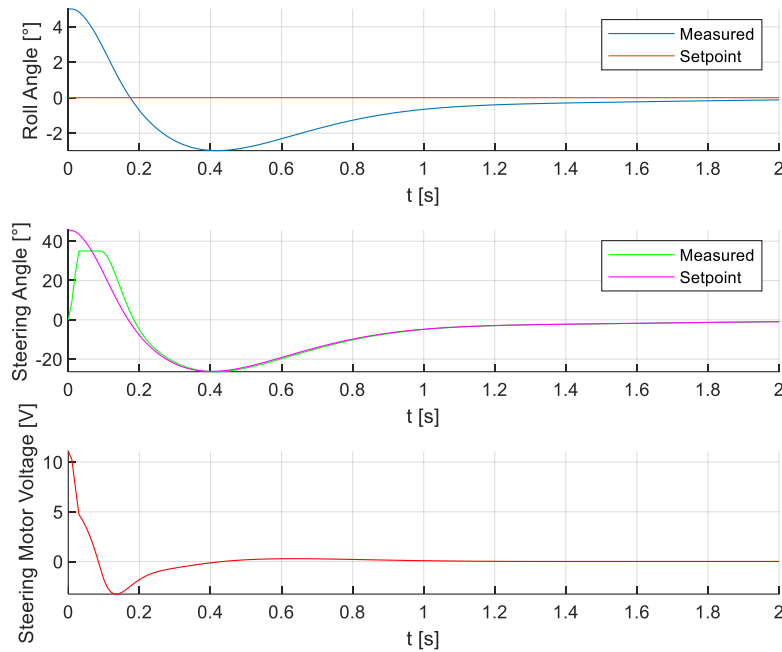


Figure 5.1: Simulated Roll and Steering Plots.

This simulation was performed at a velocity of 0.1 m s^{-1} because the model went unstable at zero velocity. The forward velocity and drive motor voltage can be seen in figure 5.2.

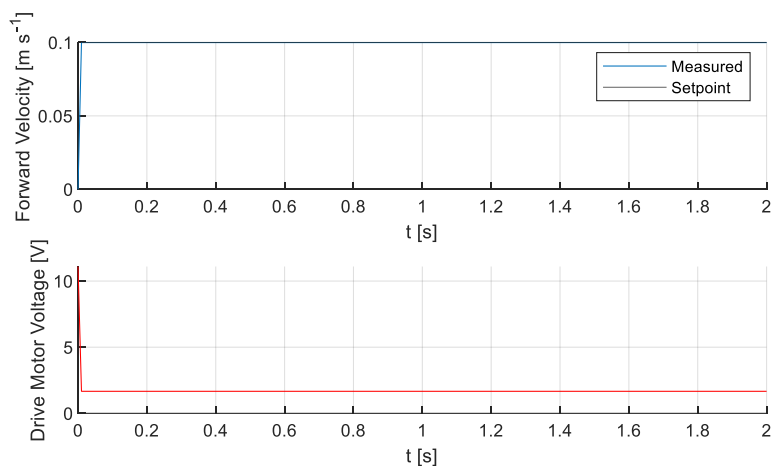


Figure 5.2: Simulated Drive Plots.

These plots will be discussed in section 6.1.

5.2. EXPERIMENTAL RESULTS

The experimental results obtained using the difference equations from subsection 4.2 were applied to the motorcycle when it had zero-velocity. The resulting plots can be seen in figure 5.3.

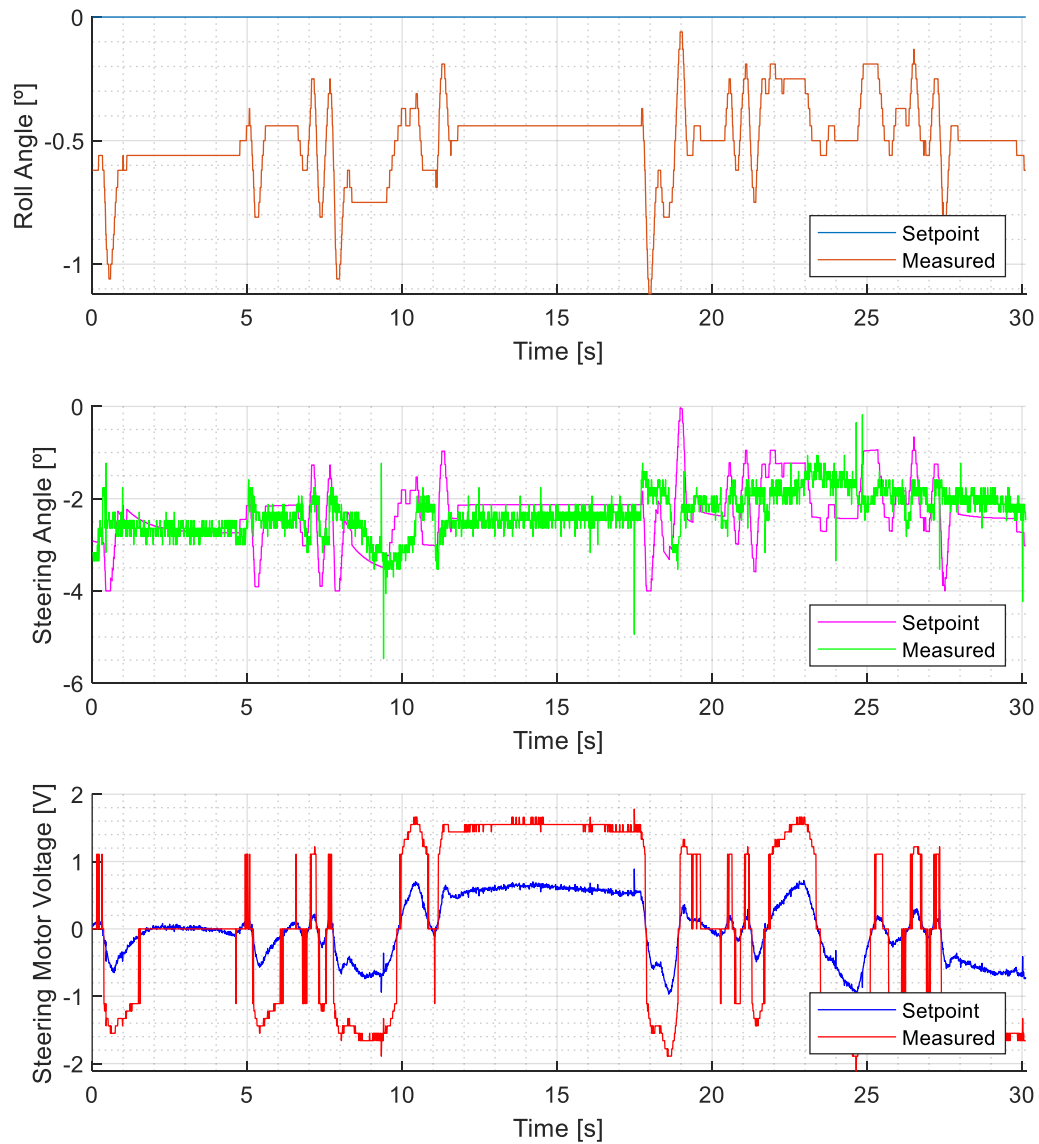


Figure 5.3: Experimental Roll and Steering Plots.

As the motorcycle was at zero velocity, no drive plot is shown. The roll and steering plots will be discussed in subsection 6.2.

6. DISCUSSION OF RESULTS

6.1. DISCUSSION OF SIMULATED RESULTS

To recap, the Simulink controllers were designed to have 0.707 damping, the roll controller had a natural frequency of 12 rad s^{-1} and the steering controller had a natural frequency of 75 rad s^{-1} .

The roll and steering angles exhibit an underdamped oscillatory response. This was expected due to the choice of 0.707 damping. An underdamped response was desirable because the average value of the steering angle was lower than if the steering trace was entirely above the time axis (overdamped). A lower average steering angle means that the motorcycle's direction of travel is altered less by steering control. Ideally, the integral of steering angle over time should be zero for no direction change. The steering motor voltage spends no time in saturation, which is desirable for control. Saturation of controller outputs is a common source of instability.

The proportional controller with a gain of 25 used with the drive system allowed for a fast rise in velocity without excessively saturating the drive motor voltage output. The fact that the roll transfer function was dependant on the motorcycle's velocity meant that a fast velocity rise was essential because the roll controller was designed to operate at the 0.1 m s^{-1} velocity setpoint.

6.2. DISCUSSION OF EXPERIMENTAL RESULTS

It was determined through an empirical approach that the controllers from the Simulink model were too fast and aggressive and caused the system to destabilise. This approach led to the controllers from subsection 4.2.

The tracking error in the roll and steering angles were most likely due to backlash in the steering gearbox and frictions that had not been accounted for in the system model. Backlash describes an imperfect connection between the teeth of the sprockets in a gearbox. This gives rise to a dead band. This means that the initial change in input does not result in a change in output until the gears mesh properly. The overshoot in the steering motor voltage was a deliberate attempt to overcome the steering dead band.

While the motorcycle did balance successfully, it was not very stable. Disturbance rejection was poor, and the control was not at a level where it would have worked with a weight (representing a person) on top of the bike. It took a significant amount of time to get the motorcycle to the stage where it would balance while stationary. This meant there was not enough remaining time to properly explore balancing while driving, hence why it has not been included in this report.

7. ETHICS AND HEALTH AND SAFETY

7.1. ETHICAL CONSIDERATIONS

Engineers Ireland and the IEEE both have codes of ethics that outline the professional responsibilities of their members [67], [68]. Both codes state that ensuring the health, safety and welfare of the public is the primary responsibility of a professional engineer. Engineers are expected to take responsibility for eliminating any safety hazard they encounter even if they have not been assigned the task of dealing with it [69]. While the ethical implications of building a model of a motorcycle may not be significant, the ethics involved in the automotive industry it represents are, especially where safety is concerned. Stabilising the roll dynamics of a motorcycle is an important ethical responsibility because it reduces the risk of low speed accidents. However, when an assistive technology like this is made available to the public it is essential to ensure it functions correctly under all possible operating conditions. The reason for this is when people start placing their trust in assistive technologies, they often become dependent on them. Putting faith in technology often results in people taking less time to practise the skills that the technology is automating for them. Should the technology fail, the risk of an accident is greater than if the technology was never used in the first place due to the reduced competency of the operator. These effects have already been seen in the automotive industry due to the widespread adoption of parking sensors and reversing cameras. There is also a risk that a wider availability of smart transport solutions may incentivise people to become inactive, leading to health issues.

Technology is getting more expensive due to the addition of non-essential features. This is most obviously seen in the rapid inflation in mobile phone prices in the last ten years. A similar technological revolution is taking place in the automotive industry with smart features such as stabilisation, autonomous driving and internet connectivity beginning to make their way into modern vehicles. The addition of these technologies is likely to increase the entry level price for purchasing a vehicle. This financial barrier could make driving inaccessible to a greater percentage of the population. For this reason, it is important that manufacturers continue producing vehicles with only basic features to keep driving affordable for the majority of the population.

Environmental awareness and sustainable practise when sourcing materials and mass-producing vehicles is becoming increasingly important. In addition to this, increasing emphasis is being placed on reducing energy consumption and emissions from vehicles during operation [28]. Any control system or smart feature, especially those responsible for mechanical actuation require energy from the vehicle's fuel reserves. For fossil fuelled vehicles it is easy to see how this presents problem, but

even in the case of electric vehicles energy consumption still results in CO₂ emissions when the electricity has not been generated via renewable sources [28].

As with most technological advancements, the addition of smart features to vehicles presents ethical concerns. The necessity of any new technology should be carefully evaluated before it is implemented. However, this should not impede the research and development of new systems. Technologies such as airbags, safety belts, traction control and pedestrian detection have prevented many serious injuries and fatalities. As always, engineers should approach design tasks with careful consideration for the best interests of society.

7.2. HEALTH AND SAFETY CONCERNS

Several health and safety concerns had to be considered prior to commencing work on this project. Potential hazards and their associated risks were identified, and risk assessment was carried out. This involved quantifying the likelihood and severity of the potential accidents presented by each hazard. Control measures were implemented to reduce the probability of accidents occurring. This subsection gives an overview of the health and safety considerations in this project but for further details the reader is referred to the risk assessment form in Appendix B.

Electricity presents a hazard anywhere it is used. It is likely that the motors used for varying the steering angle and driving the rear wheel will require medium level voltages and currents. While the voltages on the motorcycle model will not be high enough to harm someone, a short circuit could lead to arcing and a potential fire hazard. In addition, the battery will have to be charged from the mains. Mains voltage is of sufficient magnitude to inflict serious and possibly fatal injuries. To minimise risks, the charger and all components should be certified with CE marks, any electrical connections on the model should be insulated using either heat shrink tubing or insulating tape and the model should be powered off before any electrical work is carried out on it.

Lithium Polymer (LiPo) batteries present a safety hazard because if the battery is punctured, the lithium will react with oxygen in the air, resulting in a fire [70]. In addition, significant heating can occur while charging especially if the current is large [28]. In severe cases LiPo batteries have been known to catch fire while charging or due to thermal runaway [71], [72]. The possibility of a short circuit at the battery terminals also presents a fire hazard. While a small battery would not provide enough fuel to cause a serious fire, the flames could spread to surrounding objects. To mitigate the risks of battery fires it should be ensured that the correct charger is used and that the batteries are

supervised during charging. The batteries and charger should be certified with CE marks, the battery terminals should be insulated from each other and overcurrent protection should be used.

There is a danger that someone could trip over the motorcycle model while it is driving on the floor. If a fall resulted in a head injury, the outcome could be fatal. In addition, the model falling from a bench could also result in injury. The likelihood of either of these scenarios arising was low but it was decided to confine testing to a predesignated corner of the laboratory to reduce this risk further.

There is also a risk that fingers, long hair or loose clothing could get caught in the rotating parts of the model. A rapid pull from getting entangled could cause serious discomfort and possibly sprain muscles. To reduce the likelihood of this occurring, the wheels should be designed with either small gaps between spokes or as full discs so no fingers can get caught in them. Anyone working on the motorcycle should ensure that any loose items are tied back and the maximum motor torque should be limited.

Another risk with the motorcycle model is that any sharp edges or corners could cause minor cuts and scrapes. Control measures such as replacing sharp edges or corners with fillets and chamfers at the design stage and de-burring all edges after manufacture should be implemented to reduce the chances of this happening.

Power dissipation in electrical circuits causes their temperature to rise. In this project the motors and IC chips will probably heat up. Touching hot surfaces could cause burns or discomfort. It was decided to place warning stickers near components that could heat up and to allow airflow around them for cooling. The microcontroller should be programmed to limit the maximum current flow in the motor.

It is likely that some parts of this project will be 3D printed. The nozzle temperature of a 3D printer is usually in excess of 200 °C [73]. This temperature is high enough to burn through skin, albeit in localised areas due to the small size of the nozzle. Another risk of the manufacturing process is operating machinery such as milling machines and lathes. These machines present the same risks associated with rotating parts but with potentially fatal outcomes. In addition, metals can reach high temperatures during machining, presenting a risk of burns. To reduce the likelihood of workshop accidents, only trained staff members are allowed to operate the machinery and the workshop has its own risk assessment.

Working long hours on a computer could result in eye strain from looking at the monitor and repetitive strain injury from typing. In addition, poor ergonomics at the workstation could result in cramping and spinal discomfort. To avoid these scenarios, regular breaks including a short walk should be taken, the

brightness of the screen should be lowered, and IT workstations should be set up in accordance with ergonomics guidelines.

Another hazard that is often overlooked is the environment surrounding the area where the project work is being carried out. There is a risk of fires in the building and potentially dangerous equipment in the control or surrounding laboratories. To reduce these risks, all personnel in the laboratory should be familiar with their designated fire exit and assembly point. It is important to take note of any equipment or experiments in the control and surrounding laboratories and become familiar with their risk assessments.

8. SUGGESTIONS FOR FUTURE WORK

Using the mechanical model to design for control and manufacture of the motorcycle were the main focus of this project. While the author was satisfied with these areas, there is scope to improve the control algorithms used for stabilisation. Potential areas of research include, designing a non-linear state-space controller to account for the non-linearities in the roll dynamics model, further study on stabilisation while moving and improved disturbance rejection.

The broader area of motorcycle stabilisation offers plenty of scope for future study. Before stabilisation technology can be used by the public it is essential that the controller would be able to function when there are suspensions on the motorcycle. Suspensions would add damping to the steering system so either the controller will have to function in the presence of this damping or there will have to be a way to lockout the suspension during balancing. The demonstration model could be further improved by adding a motor and control loop to vary the trail length electronically and a motorised centre stand so the motorcycle could take-off and park autonomously.

Another important research is topic would be getting the stabilisation system to work when someone is riding the motorcycle. A rider would add significant mass to the system which would result in the location of the centre of mass changing. Pannier bags, and top boxes would have a similar effect. To overcome this problem, the motorcycle would need to be able to measure the mass that had been added and determine the new centre of mass. This could be achieved by measuring the vertical force going through each axle and using a computer algorithm to calculate the moments about each axle and compare them to the values when the motorcycle is not being ridden.

When the motorcycle is balancing while being ridden it would be necessary that the handlebars could be disconnected from the steering column so the rider's hands would not be rotated unexpectedly. This feature was implemented in Honda's riding assist system, but again, no details were published.

9. CONCLUSIONS

During this project a self-balancing motorcycle was modelled, simulated, designed, manufactured and controlled. The project aimed to solve problems that society has with traffic flow and parking shortages. Research has shown that up to 92 % of car drivers commute to work alone [12]. If some of these people began commuting to work on motorcycles, traffic queues could be shortened, and parts of existing car parks could be converted to more space-efficient motorcycle parking. To make widespread commuting to work via motorcycles realistic, these vehicles must first be made safe to use for the wider public. Motorcycles are typically heavy and may be difficult for a smaller rider or someone recovering from an injury to balance and support. So, to enable motorcycles to be widely used as commuter vehicles, reliable balance control must first be achieved.

Control of the roll angle of a motorcycle using the vehicle's steering angle was explored in this project. Steering control was chosen because it was the least researched and most challenging of the existing motorcycle stabilisation methods. Balancing a motorcycle at low speeds is particularly challenging because the gyroscopic stabilisation from the wheels is absent. While modelling the roll dynamics of the motorcycle, the optimum vehicle dimensions for controllability were determined. To improve steering control, a motorcycle should have a negative trail length, its centre of mass should be as low down and far forward as possible and its head tube should be as vertical as possible. A test vehicle was designed in SolidWorks based on these design criteria. The geometry from this SolidWorks model was exported to MATLAB and Simulink where controllers were designed, and transient simulations were performed. The motorcycle was manufactured using a dual-extrusion 3D printer. The controllers from MATLAB were implemented on the test vehicle. During testing, it was determined that these controllers were too aggressive and caused the system to destabilise. The difference in control requirements was most likely due to frictional forces and non-linearities that were not considered in the simulations. After several controller iterations, the motorcycle balanced while stationary however stability was low and disturbance rejection was poor. Further study into controller architectures and design could be of great benefit to this project.

The project was successful in achieving balance control of a stationary motorcycle. The author gained significant insights into systems engineering and the model-based design approach and overall, the project was a very positive experience.

10. REFERENCES

- [1] K. Dutton, S. Thompson, and B. Barraclough, *The Art of Control Engineering*, First. Boston: Addison Wesley, 1997.
- [2] Setright L. J. K., *The Guinness book of motorcycling facts and feats*, First. London: Guinness Superlatives, 1979.
- [3] "BMW Shares Vision," 2016. .
- [4] "Brand Visions." [Online]. Available: <https://www.bmwgroup.com/en/next100/brandvisions.html>. [Accessed: 05-Oct-2019].
- [5] "The BMW Motorrad VISION NEXT 100 - YouTube." [Online]. Available: <https://www.youtube.com/watch?v=oW0ShDRggt8>. [Accessed: 05-Oct-2019].
- [6] "Honda Riding Assist Motorcycle | CES 2017 | Honda." [Online]. Available: <https://www.honda.com/mobility/riding-assist>. [Accessed: 05-Oct-2019].
- [7] "Honda Riding Assist - YouTube." [Online]. Available: <https://www.youtube.com/watch?v=VH60-R8MOKo&feature=youtu.be>. [Accessed: 05-Oct-2019].
- [8] "Honda Global | Honda Riding Assist-e." [Online]. Available: <https://global.honda/products/motorshow/Tokyo2017/021.html>. [Accessed: 05-Oct-2019].
- [9] "MOTORiD | Tokyo Motor Show 2017 - Event | YAMAHA MOTOR CO., LTD." [Online]. Available: <https://global.yamaha-motor.com/showroom/event/tokyo-motorshow-2017/exhibitionmodels/motoroid/>. [Accessed: 05-Oct-2019].
- [10] Y. Yu and M. Zhao, "Steering Control for Autonomously Balancing Bicycle at Low Speed," *2018 IEEE Int. Conf. Robot. Biomimetics, ROBIO 2018*, vol. 1, pp. 33–38, 2019, doi: 10.1109/ROBIO.2018.8665347.
- [11] R. S. Sharp, S. Evangelou, and D. J. N. Limebeer, "Advances in the modelling of motorcycle dynamics," *Multibody Syst. Dyn.*, vol. 12, no. 3, pp. 251–283, 2004, doi: 10.1023/B:MUBO.0000049195.60868.a2.
- [12] "Means of Travel to Work - CSO - Central Statistics Office." [Online]. Available: <https://www.cso.ie/en/releasesandpublications/ep/p-cp6ci/p6cii/p6mtw/>. [Accessed: 27-Feb-2020].

- [13] "Lit Motors." [Online]. Available: <https://www.litmotors.com/>. [Accessed: 08-Oct-2019].
- [14] "Apple in talks to acquire self-balancing electric motorcycle firm Lit Motors too?" [Online]. Available: <https://www.cnet.com/roadshow/news/apple-takeover-talks-lit-motors-self-balancing-electric-motorcycle-report/>. [Accessed: 17-Oct-2019].
- [15] Z. Deng and H. Li, "Proceedings of the 2015 Chinese intelligent automation conference: Intelligent technology and systems," *Lect. Notes Electr. Eng.*, vol. 338, no. January, 2015, doi: 10.1007/978-3-662-46466-3.
- [16] K. J. Astrom and R. M. Murray, *Feedback Systems*. 2007.
- [17] R. C. Kavanagh and J. M. D. Murphy, "The effects of quantization noise and sensor nonideality on digital differentiator-based rate measurement," *IEEE Trans. Instrum. Meas.*, vol. 47, no. 6, pp. 1448–1456, 1998, doi: 10.1109/19.746710.
- [18] X. Bao, K. Nonami, and Z. Yu, "Combined yaw and roll control of an autonomous boat," *Proc. - IEEE Int. Conf. Robot. Autom.*, pp. 188–193, 2009, doi: 10.1109/ROBOT.2009.5152410.
- [19] "NASA - Rocking and Rolling on the Launch Pad." [Online]. Available: https://www.nasa.gov/mission_pages/constellation/ares/flighttests/areslx/AresIX_VSS.html. [Accessed: 18-Oct-2019].
- [20] M. Hübner, T. Stork, U. Becker, and E. Schnieder, "Lateral stabilization of vehicle-trailer combinations against crosswind disturbances by means of sliding control," *2008 Mediterr. Conf. Control Autom. - Conf. Proceedings, MED'08*, pp. 431–438, 2008, doi: 10.1109/MED.2008.4602075.
- [21] "How does a Helicopter fly ? - YouTube." [Online]. Available: <https://www.youtube.com/watch?v=2tdnqZgKa0E>. [Accessed: 19-Oct-2019].
- [22] "ETH Zurich - Homepage | ETH Zurich." [Online]. Available: <https://ethz.ch/en.html>. [Accessed: 18-Oct-2019].
- [23] G. Mohanarajah, "The Cubli: a cube that can jump up, balance, and 'walk,'" pp. 3722–3727, 2013.
- [24] F. Sabatino, "Quadrotor control: modeling, nonlinear control design and simulation," KTH Royal Institute of Technology, 2015.
- [25] "Segway - Simply Moving - Welcome to the Official Website of Segway Europe." [Online]. Available: <http://eu-en.segway.com/>. [Accessed: 18-Oct-2019].

- [26] "Segway - Ninebot by Segway ONE E+: Life is about balance." [Online]. Available: [http://eu-en.segway.com/products/ninebot-by-segway-one-e-\(1\)](http://eu-en.segway.com/products/ninebot-by-segway-one-e-(1)). [Accessed: 18-Oct-2019].
- [27] "RYNO Motors." [Online]. Available: <https://rynomotors.com/store/>. [Accessed: 18-Oct-2019].
- [28] J. G. Hayes and G. A. Goodarzi, *Electric Powertrain: Energy Systems, Power Electronics and Drives for Hybrid, Electric and Fuel Cell Vehicles*, First. Cork: Wiley, 2018.
- [29] T. Wang and G. Li, "Adaptive Critic Optimal Fuzzy Control for Quarter-Car Suspension Systems," *2018 Int. Conf. Information, Cybern. Comput. Soc. Syst. ICCSS 2018*, no. 2015020014, pp. 440–444, 2018, doi: 10.1109/ICSS.2018.8572428.
- [30] G. Rigatos, P. Siano, and C. Cecati, "A nonlinear H-infinity feedback control approach for asynchronous generators," *5th Int. Conf. Clean Electr. Power Renew. Energy Resour. Impact, ICCEP 2015*, vol. 1, pp. 460–465, 2015, doi: 10.1109/ICCEP.2015.7177557.
- [31] "Nissan Leaf - Intelligent Mobility | Nissan Ireland." [Online]. Available: <https://www.nissan.ie/vehicles/new-vehicles/leaf/intelligent-mobility.html#DRIVING>. [Accessed: 19-Oct-2019].
- [32] "Introducing Software Version 10.0 | Tesla." [Online]. Available: https://www.tesla.com/en_IE/blog/introducing-software-version-10-0. [Accessed: 08-Oct-2019].
- [33] M. Corno, G. Panzani, and S. M. Savaresi, "Single-Track Vehicle Dynamics Control: State of the Art and Perspective," *IEEE/ASME Trans. Mechatronics*, vol. 20, no. 4, 2015, doi: 10.1109/TMECH.2014.2382717.
- [34] K. J. Astrom, R. E. Klein, and A. Lennartsson, "Bicycle Dynamics and Control: Adapted bicycles for education and research," *IEEE Control Syst.*, vol. 25, no. 4, pp. 26–47, 2005, doi: 10.1109/MCS.2005.1499389.
- [35] O. Boubaker, "The inverted pendulum: A fundamental benchmark in control theory and robotics," *2012 Int. Conf. Educ. e-Learning Innov. ICEELI 2012*, 2012, doi: 10.1109/ICEELI.2012.6360606.
- [36] C. Yang and T. Murakami, "A study on self-balancing electric motorcycles with two-wheel steering," *2014 7th Int. Conf. Inf. Autom. Sustain. "Sharpening Futur. with Sustain. Technol. ICIAfS 2014*, pp. 1–6, 2014, doi: 10.1109/ICIAFS.2014.7069530.
- [37] "Honda's Self-Balancing Rider Assist Motorcycle is Perfect for Novice Riders | WIRED." [Online].

- Available: <https://www.wired.com/2017/01/hondas-self-balancing-motorcycle-perfect-noobs/>. [Accessed: 19-Oct-2019].
- [38] C. Yang, S. Kim, T. Nozaki, and T. Murakami, "A self-balancing performance comparison of three modes of handleless electric motorcycles," *Proceeding - 2015 IEEE Int. Conf. Ind. Informatics, INDIN 2015*, pp. 352–357, 2015, doi: 10.1109/INDIN.2015.7281760.
 - [39] "Honda Riding Assist." [Online]. Available: <http://www.slothdesign.com/technology/72-honda-riding-assist>. [Accessed: 08-Oct-2019].
 - [40] "Yamaha MOTOROiD: la moto que no se cae y que sigue tus órdenes." [Online]. Available: <https://www.todocircuito.com/noticias/16135-yamaha-motoroid:-la-moto-que-no-se-cae-y-que-sigue-tus-ordenes.html>. [Accessed: 08-Oct-2019].
 - [41] "Lit Motors patents stabilization system for the C1 - Automotorblog." [Online]. Available: <http://www.automotorblog.com/lit-motors-patents-stabilization-system-c1-52566.html>. [Accessed: 08-Oct-2019].
 - [42] "BMW Motorrad creates autonomous BMW R 1200 GS." [Online]. Available: <https://www.bmwblog.com/2018/09/12/bmw-motorrad-creates-autonomous-bmw-r-1200-gs/>. [Accessed: 19-Oct-2019].
 - [43] "First-Ever AUTONOMOUS BIKE – Demonstration – BMW R 1200 GS - YouTube." [Online]. Available: <https://www.youtube.com/watch?v=VaZITsoj0Hc>. [Accessed: 19-Oct-2019].
 - [44] R. S. Sharp, "The Stability and Control of Motorcycles," *J. Mech. Eng. Sci.*, vol. 13, no. 5, pp. 316–329, 1971, doi: 10.1243/jmes_jour_1971_013_051_02.
 - [45] J. P. Meijaard, J. M. Papadopoulos, A. Ruina, and A. L. Schwab, "Linearized dynamics equations for the balance and steer of a bicycle: A benchmark and review," *Proc. R. Soc. A Math. Phys. Eng. Sci.*, vol. 463, no. 2084, pp. 1955–1982, 2007, doi: 10.1098/rspa.2007.1857.
 - [46] A. Bonci, R. De Amicis, S. Longhi, E. Lorenzoni, and G. A. Scala, "Motorcycle's lateral stability issues: Comparison of methods for dynamic modelling of roll angle," *2016 20th Int. Conf. Syst. Theory, Control Comput. ICSTCC 2016 - Jt. Conf. SINTES 20, SACCS 16, SIMSIS 20 - Proc.*, no. Dii, pp. 607–612, 2016, doi: 10.1109/ICSTCC.2016.7790733.
 - [47] R. S. Sharp and D. J. N. Limebeer, "A Motorcycle Model for Stability and Control Analysis," *Multibody Syst. Dyn.*, vol. 6, no. 2, pp. 123–142, 2001, doi: 10.1023/A:1017508214101.
 - [48] Y. Zhang, P. Wang, J. Yi, D. Song, and T. Liu, "Stationary balance control of a bikebot," *Proc. -*

- IEEE Int. Conf. Robot. Autom.*, pp. 6706–6711, 2014, doi: 10.1109/ICRA.2014.6907849.
- [49] Q. K. Ho and C. B. Pham, “Study on Inertia Wheel Pendulum Applied to Self-Balancing Electric Motorcycle,” *Proc. 2018 4th Int. Conf. Green Technol. Sustain. Dev. GTSD 2018*, pp. 687–692, 2018, doi: 10.1109/GTSD.2018.8595698.
- [50] “[Undergraduate Project] Balancing Motorcycle - YouTube.” [Online]. Available: <https://www.youtube.com/watch?v=SUVtObDFFWY>. [Accessed: 19-Oct-2019].
- [51] D. A. Bravo, C. F. Rengifo, and J. F. Diaz, “Control of a Robotic Bicycle,” *2018 IEEE 2nd Colomb. Conf. Robot. Autom. CCRA 2018*, pp. 1–5, 2018, doi: 10.1109/CCRA.2018.8588132.
- [52] “Arduino Engineering Kit.” [Online]. Available: <https://store.arduino.cc/arduino-engineering-kit>. [Accessed: 19-Oct-2019].
- [53] A. Bonci, R. De Amicis, S. Longhi, and E. Lorenzoni, “Modeling and Simulation of the Motorcycle’s Lowside Fall,” *Procedia Manuf.*, vol. 11, no. June, pp. 2061–2068, 2017, doi: 10.1016/j.promfg.2017.07.358.
- [54] Y. Jingang, S. Dezhen, A. Levandowski, and S. Jayasuriya, “Trajectory tracking and balance stabilization control of autonomous motorcycles,” *Proc. - IEEE Int. Conf. Robot. Autom.*, vol. 2006, no. May, pp. 2583–2589, 2006, doi: 10.1109/ROBOT.2006.1642091.
- [55] J. He, M. Zhao, and S. Stasinopoulos, “Constant-velocity steering control design for unmanned bicycles,” *2015 IEEE Int. Conf. Robot. Biomimetics, IEEE-ROBIO 2015*, pp. 428–433, 2015, doi: 10.1109/ROBIO.2015.7418805.
- [56] Y. Zhang, J. Li, J. Yi, and D. Song, “Balance control and analysis of stationary riderless motorcycles,” *Proc. - IEEE Int. Conf. Robot. Autom.*, vol. 1, no. 1, pp. 3018–3023, 2011, doi: 10.1109/ICRA.2011.5979841.
- [57] C. Yang and T. Murakami, “Full-Speed Range Self-Balancing Electric Motorcycles Without the Handlebar,” *IEEE Trans. Ind. Electron.*, vol. 63, no. 3, pp. 1911–1922, 2016, doi: 10.1109/TIE.2015.2508925.
- [58] “Arduino MKR WiFi 1010 | Arduino Official Store.” [Online]. Available: <https://store.arduino.cc/arduino-mkr-wifi-1010>. [Accessed: 08-Mar-2020].
- [59] “Arduino MKR IMU Shield | Arduino Official Store.” [Online]. Available: <https://store.arduino.cc/arduino-mkr-imu-shield>. [Accessed: 08-Mar-2020].
- [60] “Arduino MKR Motor Carrier | Arduino Official Store.” [Online]. Available:

- <https://store.arduino.cc/arduino-mkr-motor-carrier>. [Accessed: 08-Mar-2020].
- [61] “22N78-311P.1001 | Portescap Brushed DC Motor, 12 W, 12 V dc, 14.8 mNm, 7280 rpm, 1.5mm Shaft Diameter | RS Components.” [Online]. Available: <https://ie.rs-online.com/web/p/dc-motors/8929120/>. [Accessed: 08-Mar-2020].
- [62] “P5-G11L82 | McLennan Servo Supplies Ovoid Gearbox, 25:1 Gear Ratio, 0.7 Nm Maximum Torque, 200rpm Maximum Speed | RS Components.” [Online]. Available: <https://ie.rs-online.com/web/p/gearboxes/0336444/>. [Accessed: 08-Mar-2020].
- [63] “Taiwan Alpha RV16AF 10K LIN 16mm Metal Case PCB Potentiometer | Rapid Online.” [Online]. Available: <https://www.rapidonline.com/taiwan-alpha-rv16af-10k-lin-16mm-metal-case-pcb-potentiometer-65-0715>. [Accessed: 09-Mar-2020].
- [64] “DealMux GA12-N20 12V 280RPM DC Gear Motor with Encoder: Amazon.co.uk: Electronics.” [Online]. Available: https://www.amazon.co.uk/gp/product/B07Y9RJKJ5/ref=ppx_yo_dt_b_asin_title_o08_s00?ie=UTF8&psc=1. [Accessed: 08-Mar-2020].
- [65] “2 x 12 volt power 8 x AA battery holder case with 2.1mm: Amazon.co.uk: Electronics.” [Online]. Available: https://www.amazon.co.uk/gp/product/B07BY3ZDDL/ref=ppx_yo_dt_b_asin_image_o06_s00?ie=UTF8&psc=1. [Accessed: 08-Mar-2020].
- [66] “OlliW’s Bastelseiten » IMU Data Fusing: Complementary, Kalman, and Mahony Filter.” [Online]. Available: <http://www.olliw.eu/2013/imu-data-fusing/>. [Accessed: 01-Mar-2020].
- [67] *Engineers Ireland Code of Ethics*. 2018.
- [68] “IEEE Code of Ethics.” [Online]. Available: <https://www.ieee.org/about/corporate/governance/p7-8.html>. [Accessed: 05-Oct-2019].
- [69] “Illinois Foundry Ethics Videos - YouTube.” [Online]. Available: <https://www.youtube.com/watch?v=n9A8-FjhArE&index=1&list=PL746AE3CCB29B64B8>. [Accessed: 05-Oct-2019].
- [70] Jensen C, “Tesla Says Car Fire Started in Battery,” *The New York Times*, pp. 1–2, 2018.
- [71] CBSNews, “Samsung recalls Galaxy Note 7 after battery explosions,” *CBSNews.com*, pp. 1–2, 2016.
- [72] Q. Wang, P. Ping, X. Zhao, G. Chu, J. Sun, and C. Chen, “Thermal runaway caused fire and

explosion of lithium ion battery,” *J. Power Sources*, vol. 208, pp. 210–224, 2012, doi: 10.1016/j.jpowsour.2012.02.038.

- [73] “3D Printing Temperatures & Printing Guidelines | Filaments.ca.” [Online]. Available: <https://filaments.ca/pages/temperature-guide>. [Accessed: 05-Oct-2019].

APPENDIX A: LINKS TO ONLINE REPOSITORIES

The files created as part of this project have been uploaded to various online repositories.

The project report, poster, Arduino code, MATLAB code and Simulink diagrams are available on GitHub at:

<https://github.com/conorhealy898/Final-Year-Project>

The project video is available on YouTube at:

<https://www.youtube.com/watch?v=fFrGl4Du1MM&t=22s>

A playlist of Motorcycle Test videos is available on YouTube at:

<https://www.youtube.com/watch?v=fm4P5YH1AP8&list=PLI1TINkoYmrWGHYhqJaogXKygd5izlUs6>

The SolidWorks and STL files for the motorcycle and IMU test rig are available on GrabCAD at:

<https://grabcad.com/library/self-balancing-motorcycle-stl-and-solidworks-files-1>

APPENDIX B: CONTINUOUS TIME PHASE LEAD CONTROLLER DESIGN CODE

```
function [K_c, zero_PL, pole_PL] = ctime_PL(sys_OL, omega_n, zeta, caption)

desired_point = zeta * omega_n * (-1 + tan(acos(zeta))*1i);
zero_PL = real(desired_point);

[pole_sys, zero_sys] = pzmap(sys_OL);
sys_r_vector = desired_point * ones(size(zero_sys)) - zero_sys;
sys_R_vector = desired_point * ones(size(pole_sys)) - pole_sys;

phase_top = pi/2;           % phase of controller zero
phase_bottom = 0;

for x = 1 : size(sys_r_vector, 1)
    phase_top = phase_top + angle(sys_r_vector(x));
end

for x = 1 : size(sys_R_vector, 1)
    phase_bottom = phase_bottom + angle(sys_R_vector(x));
end

phase_pole_PL = pi + phase_top - phase_bottom;
pole_PL = real(desired_point) - imag(desired_point)/tan(phase_pole_PL);

PL = tf([1 -zero_PL], [1, -pole_PL]);
sys_PL = series(PL, sys_OL);
K_c = abs(real(1/ evalfr(sys_PL, desired_point)));

figure
rlocusplot(sys_PL); title(caption);
hold on;
pole = rlocus(sys_PL, K_c);
plot(real(pole), imag(pole), 'mx', 'Markersize', 10);
hold off;
sgrid;
end
```

APPENDIX C: MATCHED POLE ZERO PHASE LEAD EMULATION CODE

```
function [K_c_d, zero_PL_d, pole_PL_d] = ...
    MPZ_PL(K_c_a, zero_PL_a, pole_PL_a, T_s, c_time_sys_OL, caption)

zero_PL_d    = exp(zero_PL_a * T_s);
pole_PL_d    = exp(pole_PL_a * T_s);

DCG_a_PZ     = (zero_PL_a / pole_PL_a);
DCG_d_PZ     = (1 - zero_PL_d) / (1 - pole_PL_d);

K_c_d        = K_c_a * DCG_a_PZ / DCG_d_PZ;

PL_d         = tf([1 -zero_PL_d], [1, -pole_PL_d], T_s);

d_time_sys_OL = c2d(c_time_sys_OL, T_s, 'zoh');
sys_PL_d      = series(PL_d, d_time_sys_OL);

figure
rlocusplot(sys_PL_d);
ylim([-1.2, 1.2]);
hold on;
pole = rlocus(sys_PL_d, K_c_d);
plot(real(pole), imag(pole), 'mx', 'Markersize', 10);
title(caption);
hold off;
zgrid;
end
```

APPENDIX D: DISCRETE TIME PHASE LEAD CONTROLLER DESIGN CODE

```
function [K_c, zero_PL, pole_PL] = ...
    dtime_PL(c_time_sys_OL, omega_n, zeta, T_s, caption)

d_time_sys_OL = c2d(c_time_sys_OL, T_s, 'zoh');
[pole_sys, zero_sys] = pzmap(d_time_sys_OL);

desired_point = zeta * omega_n * (-1 + tan(acos(zeta))*1i);
desired_point = exp(desired_point * T_s);
zero_PL = real(desired_point);

sys_r_vector = desired_point * ones(size(zero_sys)) - zero_sys;
sys_R_vector = desired_point * ones(size(pole_sys)) - pole_sys;

r_vector = [sys_r_vector; desired_point - zero_PL];

phase_top = 0;
phase_bottom = 0;

for x = 1 : size(r_vector, 1)
    phase_top = phase_top + angle(r_vector(x));
end

for x = 1 : size(sys_R_vector, 1)
    phase_bottom = phase_bottom + angle(sys_R_vector(x));
end

phase_pole_PL = pi + phase_top - phase_bottom;
pole_PL = real(desired_point) - imag(desired_point)/tan(phase_pole_PL);

PL = tf([1 -zero_PL], [1, -pole_PL], T_s);
sys_PL = series(PL, d_time_sys_OL);
K_c = abs(real(1/ evalfr(sys_PL, desired_point)));

figure
rlocusplot(sys_PL);
hold on;
pole = rlocus(sys_PL, K_c);
plot(real(pole), imag(pole), 'mx', 'Markersize', 10);
title(caption);
hold off;
zgrid;
end
```


APPENDIX E: RISK ASSESSMENT

| Area/ Activity: | <i>Design an Stabilisation of a Motorcycle Model</i> | Assessment By: | <i>Conor Healy</i> | | | | | |
|---|--|-------------------------|--------------------|---------------------|--|---------------------|----------|-----------|
| Location: | <i>Control Laboratory & Mechanical Workshop, Electrical and Electronic Engineering Building, UCC.</i> | Assessment Date: | 30-09-2019 | Review Date: | 4-10-2019 | | | |
| Hazard | Risk | Risk Rating | | | Control Measures | Revised Risk | | |
| | | L | S | RR | | L | S | RR |
| <i>Electricity – medium voltages and currents for motor control, mains connection for battery charging.</i> | <i>Fire hazards from short circuits, electric shocks, burns and discomfort.</i> | 2 | 3 | 6 | <ul style="list-style-type: none"> All components and chargers certified with CE marks. Connections insulated with heat shrink tubing or electrical tape. Power disconnected before any wiring alterations or charging connections are made. | 1 | 3 | 3 |
| <i>LiPo batteries.</i> | <i>Fire due to puncture of the battery or a charging malfunction.</i> <i>Fire hazards from short circuits at the battery terminals.</i> | 1 | 3 | 3 | <ul style="list-style-type: none"> Design the motorcycle model so the battery is in a concealed location. Ensure the correct power supply is used for charging. The batteries and charger should be certified with CE marks. Only charge batteries when someone is available to watch them. Ensure that a suitable fire extinguisher is in the vicinity. Insulate the battery terminals are from each other. Ensure overcurrent protection is used. | 1 | 3 | 3 |
| <i>The motorcycle model.</i> | <i>Slips, trips and falls due to the motorcycle model.</i> <i>Injury if the model falls from a height.</i> | 1 | 3 | 3 | <ul style="list-style-type: none"> Confine motorcycle testing to a predesignated floor area in the corner of the laboratory. Ensure people stay out of the area during testing. | 1 | 3 | 3 |

| Area/ Activity: | <i>Design an Stabilisation of a Motorcycle Model</i> | Assessment By: | <i>Conor Healy</i> | | | | | |
|---------------------------------|---|-------------------------|--------------------|---------------------|---|---------------------|----------|-----------|
| Location: | <i>Control Laboratory & Mechanical Workshop, Electrical and Electronic Engineering Building, UCC.</i> | Assessment Date: | 30-09-2019 | Review Date: | 4-10-2019 | | | |
| Hazard | Risk | Risk Rating | | | Control Measures | Revised Risk | | |
| | | L | S | RR | | L | S | RR |
| <i>Rotating parts.</i> | <i>Pinching of fingers and entanglement with hair or loose clothing.</i> | 2 | 2 | 4 | <ul style="list-style-type: none"> Design the motorcycle to have either disc wheels or make the gaps between the spokes too small for a finger to get caught in them. Ensure that any long hair or loose clothing is tied up while working on the model. Constrain the maximum output torque of the motor. | 1 | 2 | 2 |
| <i>Sharp edges and corners.</i> | <i>Minor cuts or scrapes.</i> | 2 | 1 | 2 | <ul style="list-style-type: none"> Replace and sharp corners or edges with fillets or chamfers at the design stage. Check each part after manufacture and remove any burrs that might be present. | 1 | 1 | 1 |
| <i>Heating of components.</i> | <i>Burns or discomfort.</i> | 2 | 1 | 2 | <ul style="list-style-type: none"> Place warning stickers near any components (e.g. motors or IC chips) that may get hot during operation. Design the motorcycle model to allow airflow around any component that has the potential to heat up. Program the microcontroller to limit the maximum current allowed to flow in the motor. | 1 | 1 | 1 |
| <i>Tools and machinery.</i> | <i>Burns from the 3D printer nozzle or machined surfaces.</i> <i>Fingers, hair or loose clothing getting caught in moving parts.</i> | 2 | 3 | 6 | <ul style="list-style-type: none"> Ensure anyone using tools or machinery has had the correct training for the task. Any machinery used should be certified with CE marks. Tie back any long hair or loose clothing while operating machinery. Correct use of PPE. | 1 | 3 | 3 |

| Area/ Activity: | <i>Design an Stabilisation of a Motorcycle Model</i> | Assessment By: | <i>Conor Healy</i> | | | | | |
|-------------------------------------|---|-------------------------|--------------------|---------------------|---|---------------------|----------|-----------|
| Location: | <i>Control Laboratory & Mechanical Workshop, Electrical and Electronic Engineering Building, UCC.</i> | Assessment Date: | 30-09-2019 | Review Date: | 4-10-2019 | | | |
| Hazard | Risk | Risk Rating | | | Control Measures | Revised Risk | | |
| | | L | S | RR | | L | S | RR |
| <i>Computer work.</i> | <i>Eye strain from the monitor, repetitive strain injury from typing, muscle injury or discomfort due to poor ergonomics.</i> | 2 | 1 | 2 | <ul style="list-style-type: none"> Take regular breaks from working, including a short walk. Lower the brightness of the screen and/ or enable the night-light setting. Set up IT workstations in accordance with ergonomics guidelines. | 1 | 1 | 1 |
| <i>The surrounding environment.</i> | <i>Fires in the building, potentially dangerous equipment and projects in the control and surrounding laboratories.</i> | 2 | 3 | 6 | <ul style="list-style-type: none"> Ensure all personnel in the laboratory are familiar with their designated fire exit and assembly point. Take note of any equipment or experiments in the control and surrounding laboratories and become familiar with their risk assessments. | 1 | 3 | 3 |

Declaration:

I declare that I have read the above risk assessment and I fully understand the hazards, risks and associated controls. I am fully aware of my roles and responsibilities in relation to the activity.

| Name: | Signature: | Date: |
|------------------|--|------------------------------|
| Conor Healy |  | 4 th October 2019 |
| Gordon Lightbody |  | 4 th October 2019 |

APPENDIX F: LOGBOOK

SEMESTER 1 WEEK 1

Date: 9th September 2019 – 13th September 2019.

Project Progress and Achievements

Project Planning and Organisation

- Read the final year project (FYP) handbook to understand the project goals.
- Got a laboratory notebook (number -01-19/20) from the departmental operative.
- Arranged a meeting with Dr. Gordon Lightbody about undertaking a control project.
- Met with Dr. Lightbody on Thursday to discuss the scope of the project, decide on a title and fill in the project allocation form (see laboratory notebook -01-19/20 pages 1-4).
- Made an ordered list of the steps in the design process (see laboratory notebook -01-19/20 pages 5 and 6). These steps would each have chapters in the final report.

Reports

- Made template documents for the preliminary and final reports in Microsoft Word. Both templates included a cover page and chapter titles.
- Made a template for the seminar presentation in Microsoft PowerPoint.

Work Planned for Next Week

- Research systems that are balanced (e.g. ETH Zurich Cube, 2-wheel inverted pendulum, etc.).
- Research specifications of the Arduino MKR boards, IMU Shield and Motor Carrier.
- Attend EE4050 seminars on Tuesday and Wednesday.
- Begin modelling the dynamics of the motorcycle system.
- Watch the ethics videos recommended by the module coordinator in preparation for the upcoming ethics assignment.

SEMESTER 1 WEEK 2

Date: 16th September 2019 – 20th September 2019.

Project Progress and Achievements

Reports

- Printed and read the guide for the ethical reasoning case study.
- Downloaded the Engineers Ireland Code of Ethics and the IEEE Code of Conduct to learn about an engineer's ethical responsibilities.
- Watched the engineering ethics videos recommended by the module coordinator in preparation for the ethical reasoning assignment (see laboratory notebook - 01 - 2019 pages 15-18).
- Began working on the ethical reasoning assignment.

System Modelling

- Downloaded journal articles about motorcycle stability and dynamics. These papers gave descriptions of the torques acting on the motorcycle system. Of particular note was Robin Sharp's 1971 motorcycle model [1].

Component Selection

- Researched the Arduino MKR boards, MKR IMU shield and MKR motor carrier. Decided to use the MKR 1010 board because it has BLE (Bluetooth Low Energy) capability. This will allow the motorcycle to be connected to a smartphone.

EE4050 BE Project Seminars

- Attended the EE4050 Project Management seminar delivered by Richard Kavanagh on Tuesday (see laboratory notebook -01-19/20 page 10).
- Attended the EE4050 Information Literacy seminar delivered by Anita Wilcox on Wednesday (see laboratory notebook -01-19/20 pages 11-14).

Work Planned for Next Week

- Finish writing and submit the ethical reasoning case study.
- Continue searching the literature for information about systems that are balanced/ stabilised.

[1] R. S. Sharp, 'The stability and control of motorcycles', *Journal Mechanical Engineering Science*, Vol. 3, No. 5, pp. 316-329, 1971.

SEMESTER 1 WEEK 3

Date: 23rd September 2019 – 27th September 2019.

Project Progress and Achievements

Project Planning and Organisation

- Had a discussion with Dr. Lightbody on Thursday to discuss the key topics for the literature review and a mechanical model for the motorcycle system (see laboratory notebook -01-19/20 pages 24, 25).

Reports

- Finished and submitted the ethical reasoning case study.
- Added subheadings to the final report template.
- Began writing the introduction and objectives section and the ethics and health and safety section.

System Modelling

- Found a journal paper that modelled a bicycle with the steering as the only control input [2]. The model included a variable trail length and should be suitable for this project.

EE4050 BE Project Seminars

- Attended the EE4050 Health & Safety – Risk Assessment seminar delivered by Brendan O’Driscoll on Tuesday (see laboratory notebook -01-19/20 pages 19-22).
- Attended the EE4050 Entrepreneurship seminar delivered by Gillian Barrett on Wednesday (see laboratory notebook -01-19/20 page 23).

Work Planned for Next Week

- Finish writing the introduction and objectives section and the ethics and health and safety section.
- Begin writing the literature review.

[2] Y. Yu, M. Zhao, ‘Steering Control for Autonomously Balancing Bicycle at Low Speed’, *2018 IEEE International Conference on Robotics and Biomimetics*, pp. 33-38, 2018.

SEMESTER 1 WEEK 4

Date: 30th September 2019 – 4th October 2019.

Project Progress and Achievements

Project Planning and Organisation

- Organised a weekly meeting time with Dr. Lightbody on Fridays from 10 am to 11 am.
- Obtained a SolidWorks Student Edition licence and installed it. The software is now ready for designing the physical model.
- Met with Michael O'Shea and Tim Power in the manufacturing workshop to see what tools and machines they had and organise getting parts made.
- Met with Hilary Mansfield to discuss sensors, microcontrollers and ordering parts.
- Met with Dr. Lightbody. During the meeting, the risk assessment was reviewed and the design of the motorcycle was discussed (see laboratory notebook -01-19/20 page 27).

Reports

- Wrote the majority of the introduction and objectives section (excluding a description of stabilisation systems as this will summarise the findings of the literature review).
- Completed the risk assessment form.
- Wrote the ethics and health and safety section of the project report.
- Began working on the literature review.
- Reviewed and altered the risk assessment with Dr. Lightbody. The assessment form has been signed.

EE4050 BE Project Seminars

- Attended the EE4050 Report Writing & Lab Notebooks seminar delivered by Kevin McCarthy on Tuesday (see laboratory notebook -01-19/20 page 26).

Work Planned for Next Week

- Make substantial progress on the literature review.
- Begin making a list of parts for ordering.

SEMESTER 1 WEEK 5

Date: 7th October 2019 – 11th October 2019.

Project Progress and Achievements

Project Planning and Organisation

- No project meeting this week due to a Science Foundation Ireland (SFI) review.

Reports

- Installed the Mendeley software for managing citations.
- Wrote the literature review excluding subsections about controller architectures for stabilisation and sensors and microcontroller platforms.

System Simulation

- Began working on building a model for the motorcycle in Simulink. Two models were built, one for when the motorcycle is stationary and the other for when the motorcycle is moving at constant velocity (see laboratory notebook -01-19/20 pages 34-41).

EE4050 BE Project Seminars

- Attended the EE4050 Communication Skills seminar delivered by Alan Morrison on Tuesday (see laboratory notebook -01-19/20 pages 28-31).
- Attended the EE4050 Data Analysis & Presentation seminar delivered by Paul Leahy on Wednesday (see laboratory notebook -01-19/20 pages 32, 33).

Work Planned for Next Week

- Complete the literature review.
- Finish building the preliminary Simulink models.

SEMESTER 1 WEEK 6

Date: 14th October 2019 – 18th October 2019.

Project Progress and Achievements

Project Planning and Organisation

- Project meeting with Dr. Lightbody on Friday. Some important recommendations from the meeting were to simplify the physical motorcycle by manually adjusting the trail length and eliminating the motorised centre stand. It was also recommended that a PID controller be used for the initial simulations and that a state space controller could be designed after Christmas when the EE4002 Control Engineering module has been completed.

Reports

- Completed the literature review.
- Formed the preliminary report based on what had been written in the final thesis. The summary of achievements to date and project work plan will be written closer to the date of submission so they are as up to date as possible.

System Simulation

- Made a block diagram showing how the various motorcycle subsystems would interconnect within the motorcycle system for the constant velocity model (see laboratory notebook -01-19/20 pages 44-46).

EE4050 BE Project Seminars

- Attended the EE4050 Business Model Generation seminar delivered by Pdraig Cantillon-Murphy on Tuesday (see laboratory notebook -01-19/20 page 42).
- Attended the EE4050 Introduction to Intellectual Property Creation and Protection seminar delivered by Pdraig Cantillon-Murphy on Wednesday (see laboratory notebook -01-19/20 page 43).

Work Planned for Next Week

- Combine the subsystems designed in the logbook to form a comprehensive model of the motorcycle's dynamics in Simulink.
- Identify the system behaviour and design a PID controller for preliminary simulations.

SEMESTER 1 WEEK 7

Date: 21st October 2019 – 25th October 2019.

Project Progress and Achievements

Project Planning and Organisation

- No project meeting this week.

System Simulation

- Made a Simulink model of the motorcycle including, velocity, steering and roll subsystems. Separate Simulink diagrams for each subsystem were created to simplify system identification (see laboratory notebook -01-19/20 pages 44-57).
- Proposed preliminary classical controller architectures for both the forward velocity and roll angle. It was decided to use a cascade controller for the roll dynamics (see laboratory notebook -01-19/20 pages 58, 59).
- A MATLAB script was written to initialise variables in the workspace and plot useful data.
- Began system identification of the steering subsystem.

Motorcycle Design

- Sketched some initial designs for the Motorcycle model and a stand to hold it when it is not in use (see laboratory notebook -01-19/20 pages 60-63).

Work Planned for Next Week

- Finish the system identification of the three subsystems.
- Design preliminary controllers for the motorcycle in Simulink.
- Build the Arduino MKR 1010 board, MKR IMU Shield and MKR Motor Carrier in SolidWorks.

SEMESTER 1 WEEK 8

Date: 29th October 2019 – 1st November 2019, (public holiday on Monday 28th October).

Project Progress and Achievements

Project Planning and Organisation

- Project meeting on Friday where the results of the system identification tests, preliminary controller designs using the root locus method and potential controller architectures were discussed.

Reports

- Proof read the literature review.
- Completed the preliminary report.

System Simulation

- Completed the system identification of the steering system, drive system and roll dynamics.
- Obtained bode plots, pole-zero maps and transfer function models for each of the subsystems.

Motorcycle Design

- Analysed a linear transfer function model of the motor cycle roll dynamics obtained from [3] to determine what motorcycle geometry would be most suitable for stabilisation via steering control (see laboratory notebook -01-19/20 pages 64-66).
- Began designing a motorcycle model with geometry to maximise the sensitivity of the roll angle to the steering angle (see laboratory notebook -01-19/20 pages 67-69).

Work Planned for Next Week

- Submit the preliminary report.
- Design preliminary controllers for the motorcycle in Simulink.
- Build the Arduino MKR 1010 board, MKR IMU Shield and MKR Motor Carrier in SolidWorks.

SEMESTER 1 WEEK 9

Date: 4th November 2019 – 8th November 2019.

[3] Y. Yu, M. Zhao, 'Steering Control for Autonomously Balancing Bicycle at Low Speed', *2018 IEEE International Conference on Robotics and Biomimetics*, pp. 33-38, 2018.

Project Progress and Achievements

Project Planning and Organisation

- Less progress made than usual this week due to a Photonics exam on Thursday.
- No project meeting this week.

Reports

- Made block diagrams for the proposed motorcycle stabilisation system and a basic digital control system (see figures 2.1 and 3.2 in the preliminary report).
- Printed a draft copy of the preliminary report so Dr. Lightbody could check if its formatting was satisfactory.
- Proofread the preliminary report.

System Simulation

- Began designing the preliminary controllers for the motorcycle in Simulink.

Work Planned for Next Week

- Continue designing the preliminary controllers for the motorcycle in Simulink.
- Build the Arduino MKR 1010 board, MKR IMU Shield and MKR Motor Carrier in SolidWorks.

SEMESTER 1 WEEK 10

Date: 11th November 2019 – 15th November 2019.

Project Progress and Achievements

Project Planning and Organisation

- No project meeting this week.

Reports

- Submitted the preliminary report.

System Modelling

- Derived linearised transfer functions for the roll dynamics, steering dynamics and forward dynamics subsystems (see laboratory notebook -01-19/20 pages 72-78).

System Simulation

- Began writing a MATLAB script to calculate the numerical values for these transfer functions and plot root locus diagrams with the preliminary controllers.

Motorcycle Design

- Built a basic model of the Arduino MKR 1010 board, MKR IMU Shield and MKR Motor Carrier in SolidWorks. This model was satisfactory for designing the motorcycle but more detail will be added for aesthetics at a later date.

Work Planned for Next Week

- Finish writing the MATLAB script for designing the preliminary controllers.
- Calculate the torque and speed requirements for the steering and drive motors.
- Begin working on a component list so parts for the project can be ordered.

SEMESTER 1 WEEK 11

Date: 18th November 2019 – 22nd November 2019.

Project Progress and Achievements

Project Planning and Organisation

- No project meeting on Friday because a discussion after class on Thursday covered the important points for the week.

System Modelling

- Derived normalised forms of the linearised transfer functions (see laboratory notebook -01-19/20 pages 78, 79).
- Factorised the linearised transfer functions (see laboratory notebook -01-19/20 pages 80, 81).
- Compared the numerical values of the derived transfer functions and the ones obtained from the linear analysis tool in MATLAB (see laboratory notebook -01-19/20 pages 82, 83). There were some discrepancies for the steering and drive systems. The source of these errors will be determined after the winter exams have been completed as understanding them is not essential for choosing the motors.

System Simulation

- Wrote a MATLAB function that calculate the controller parameters and plots the root locus for a continuous time phase-lead compensated system using the method described in chapter 5 of the EE3016 notes (controller zero placed on the real axis directly under the desired point, controller pole positioned on the real axis so the phase is $-\pi$ at the desired point, controller gain chosen so the magnitude of the open loop transfer function is 1 at the desired point).
- Wrote similar functions for continuous time PI, PD and PID controllers and discrete time phase lead, PI, PD and PID controllers. For the discrete time controllers, the method described in chapter 2 of the EE4002 notes was used (same as above but using the z-domain instead of the s-domain). For the PID controllers there was an option to use a double controller zero or to fix one zero on the real axis under the desired point and use the other to satisfy the $-\pi$ phase requirement.

Work Planned for Next Week

- Choose the steering and drive motors.

SEMESTER 1 WEEK 12

Date: 25th November 2019 – 29th November 2019.

Project Progress and Achievements

- No project work due to upcoming exams.

CHRISTMAS PERIOD

Date: 23rd December 2019 – 10th January 2020, (no project work during winter exam period).

Project Progress and Achievements

Project Planning and Organisation

- Project Meeting on the 8th of January to discuss the progress that had been made during the Christmas period.
- Ordered parts for the project through the university.

System Simulation

- Completed the design of the preliminary controllers.

Motorcycle Design

- Choose appropriate components for the motorcycle based on the results from the preliminary control simulations.
- Designed a physical model for the motorcycle on SolidWorks.

Motorcycle Manufacture

- Began 3D printing the various parts of the motorcycle model.

Work Planned for Next Week

- Continue 3D printing the parts of the motorcycle model.

SEMESTER 2 WEEK 1

Date: 13th January 2020 – 17th January 2020.

Project Progress and Achievements

Project Planning and Organisation

- Less progress made this week due to a control assignment deadline.
- Obtained the parts for the project from the university.

Motorcycle Design

- Redesigned the battery holder for the motorcycle as the preferred battery pack was not available for shipping to Ireland.

Motorcycle Manufacture

- Continued 3D printing the various parts of the motorcycle model.

Work Planned for Next Week

- Finish 3D printing the motorcycle parts.
- Weigh each individual part of the motorcycle so SolidWorks can calculate the location of the centre of mass.
- Assemble the motorcycle.
- Design a centre stand to prevent the motorcycle from falling on its side when testing the self-balancing algorithm.

SEMESTER 2 WEEK 2

Date: 20th January 2020 – 24th January 2020.

Project Progress and Achievements

Project Planning and Organisation

- Arranged a weekly meeting time for 4 pm on a Wednesday.
- Discussed the control of the motorcycle and the need for building an IMU test rig.

Motorcycle Manufacture

- Finished 3D printing the parts for the motorcycle model.
- 3D printed a spare set of tires.

IMU Test Rig

- Designed an IMU test rig in SolidWorks.
- 3D printed the parts for the IMU test rig.

Work Planned for Next Week

- Weigh each individual part of the motorcycle so SolidWorks can calculate the location of the centre of mass.
- Assemble the motorcycle.
- Design a centre stand to prevent the motorcycle from falling on its side when testing the self-balancing algorithm (need to know where the centre of mass is first).

SEMESTER 2 WEEK 3

Date: 27th January 2020 – 31st January 2020.

Project Progress and Achievements

Project Planning and Organisation

- Project meeting as normal.

Motorcycle Design

- Weighed each component of the motorcycle.
- Calculated the centre of mass of the motorcycle in SolidWorks.

Motorcycle Manufacture

- 3D printed the centre stand.
- Made the axles.
- Began assembling the motorcycle.

IMU Test Rig

- Assembled the IMU test rig.

Work Planned for Next Week

- Simulate the system with the calculated centre of mass value to ensure that the 3D printed motorcycle will be controllable.

SEMESTER 2 WEEK 4

Date: 3rd February 2020 – 7th February 2020.

Project Progress and Achievements

Project Planning and Organisation

- Project meeting as usual.
- Less progress this week due to focusing on a short-term project.

System Simulation

- Simulated the system with the calculated centre of mass to ensure that the 3D printed motorcycle model will be controllable.

Work Planned for Next Week

- Prepare slides and practice for the presentation on Friday the 14th of February.
- Finish assembling the motorcycle before the presentation.

SEMESTER 2 WEEK 5

Date: 10th February 2020 – 14th February 2020.

Project Progress and Achievements

Project Planning and Organisation

- No project meeting this week due to an appointment.
- This week was focused on the project presentation.

Project Presentation

- Prepared slides for the presentation.
- Rehearsed the presentation.
- Delivered the presentation on Friday the 14th of February.

Motorcycle Manufacture

- Finished assembling the motorcycle for the presentation.

Work Planned for Next Week

- Test the IMU with the IMU test rig.
- Attach the steering gearbox sprocket to the steering motor.

SEMESTER 2 WEEK 6

Date: 17th February 2020 – 21st February 2020.

Project Progress and Achievements

Project Planning and Organisation

- Project meeting where the combined system simulation, IMU test rig and re-designs were discussed.
- Ordered 70 mm diameter seals to use as a belt drive. The rubber belt that was being used initially stretched too easily, resulting in poor power transfer to the rear wheel.

System Simulation

- Combined the steering, roll and drive systems into a single Simulink diagram to ensure that the motorcycle could balance with changing velocity values.

Motorcycle Design

- The plastic steering potentiometer was too weak and cracked so it was necessary to re-design the upper body and head cap to accommodate a stronger metal potentiometer.
- The wheels rocked laterally on their axles, so it was decided to redesign the wheels to include bearings and steel axles. Lateral rocking would have resulted in a significant dead-band and impeded the action of the steering controller.

Motorcycle Manufacture

- Collected bearings from the mechanical workshop to use in the re-designed wheels.
- Arranged to have a sprocket mounted onto the steering motor shaft in the mechanical workshop.
- 3D printed a new upper forks to accommodate the new steering potentiometer.

IMU Test Rig

- Tested the IMU and determined that it had in-built sensor fusion.

Work Planned for Next Week

- 3D print the new upper body and head cap.
- Update the literature review for the final report.

SEMESTER 2 WEEK 7

Date: 24th February 2020 – 28th February 2020.

Project Progress and Achievements

Project Planning and Organisation

- No project meeting this week due to 3D printing problems.

Motorcycle Manufacture

- 3D printed new wheels and pulleys to accommodate the bearings and new drive-belt.
- 3D printed a new upper body of the motorcycle and a new head cap to accommodate the new potentiometer. Green plastic was used due to a shortage of red.
- Gave a working drawing for the axles into the mechanical workshop and collected the manufactured axles.
- Assembled the new wheels with their bearings and axles.
- Assembled the forks with the new front wheel and upper forks.

Reports

- Updated the literature review for the final report based on corrections from the preliminary report and more recent research.

Work Planned for Next Week

- Assemble the motorcycle with the re-designed parts.
- Wire the motorcycle.
- Continue working on the final report.

SEMESTER 2 WEEK 8

Date: 2nd March 2020 – 6th March 2020.

Project Progress and Achievements

Project Planning and Organisation

- Project meeting as usual.

Motorcycle Manufacture

- Assembled the motorcycle with the new parts.

IMU Test Rig

- Soldered the potentiometer in the IMU test rig.
- Compared the output from the IMU and the potentiometer to determine the IMU's accuracy.

Reports

- Added the logbook to the final report.
- Added IMU testing to the final report.

Work Planned for Next Week

- Write Arduino code to control the motorcycle.

SEMESTER 2 WEEK 9

Date: 9th March 2020 – 13th March 2020.

Project Progress and Achievements

Project Planning and Organisation

- Project meeting where the Arduino code was discussed.
- The university was closed due to COVID-19. This meant that further meetings with Dr. Lightbody would not be possible.

Motorcycle Control

- Wrote Arduino code to control the motorcycle.
- Began testing the control algorithm on the motorcycle. No tests were successful.

Work Planned for Next Week

- Continue tuning the motorcycle controllers.

SEMESTER 2 WEEK 10

Date: 16th March 2020 – 20th March 2020, (public holiday on Tuesday 17th March).

Project Progress and Achievements

Project Planning and Organisation

- Frequent communication with Dr. Lightbody to try improving the control to a level where the motorcycle would balance.

Motorcycle Control

- Continued tuning the phase lead controllers to achieve stability while balancing the motorcycle.

Reports

- Began working on the project poster.

Work Planned for Next Week

- Complete and submit the project poster.
- Complete and submit the project video.

SEMESTER 2 WEEK 11

Date: 23rd March 2020 – 27th March 2020.

Project Progress and Achievements

Motorcycle Manufacture

- 3D printed new wheels with a different tire profile to improve the system's stability.

Motorcycle Control

- Continued tuning the controllers for the motorcycle.
- Achieved stationary balancing of the motorcycle.

Reports

- Completed and submitted the project poster.
- Completed and submitted the project video.

Work Planned for Next Week

- No project work planned for next week due to deadlines for other modules.

SEMESTER 2 WEEK 12

Date: 30th March 2020 – 3rd April 2020.

Project Progress and Achievements

Project Planning and Organisation

- No project work this week due to focusing on other assignments.

Work Planned for Next Week

- Complete the final report.
- Upload files to online repositories.

EASTER WEEK 1

Date: 6th April 2020 – 10th April 2020.

Project Progress and Achievements

Project Planning and Organisation

- Uploaded the Arduino and MATLAB code and the project poster and report to GitHub.
- Uploaded the project video and motorcycle test videos to YouTube.
- Uploaded the SolidWorks and STL files for the Motorcycle and IMU Test Rig to GrabCAD.

Reports

- Completed and submitted the final report. This included writing about the simulation, manufacture and experimental implementation.